

Supplementary Information

Second-order programming the synthesis of metal-organic frameworks

Mitchell G. Fishburn^a, Dayne R. Skelton^a, Shane G. Telfer^b, Pawel Wagner^c, Christopher Richardson^{*a}

^a School of Chemistry and Molecular Bioscience, University of Wollongong, Wollongong NSW 2522, Australia

^b MacDiarmid Institute for Advanced Materials and Nanotechnology, Institute of Fundamental Sciences, Massey University, Palmerston North 4442, New Zealand

^c Intelligent Polymer Research Institute, University of Wollongong, Wollongong NSW 2522, Australia

Table of Contents

1	General Experimental	2
2	Synthesis and Spectra of Ligands and Precursors	4
3	Synthesis of Metal-organic Frameworks	17
4	Control Reactions	23
5	Powder X-ray Diffraction	26
6	Single Crystal X-ray Crystallography	28
7	TG—DSC data.....	42
8	Gas Adsorption Isotherms and Surface Area Calculations.....	49

1 General Experimental

All chemicals used were of analytical grade and purchased from either Sigma Aldrich or Ajax Finechem Pty Ltd. Low water content DMF was purchased from VWR.

^1H NMR and ^{13}C NMR spectra were obtained using a Bruker Ascend 400 MHz or Avance 500 MHz spectrometers and referenced to the residual protio peak at δ 2.50 ppm in $\text{DMSO-}d_6$ or δ 7.26 ppm in CDCl_3 . ^{13}C NMR spectra were referenced to the solvent peaks at 39.52 ppm in $\text{DMSO-}d_6$ or 77.16 in CDCl_3 . ^1H NMR analysis was performed on MOF samples (~10 mg) digested by adding 35% DCl in D_2O (3 or 3.5 μL) and $\text{DMSO-}d_6$ (500 μL) and sonicated until a solution was obtained.

PXRD patterns were obtained using a GBC-MMA X-Ray diffractometer using $\text{Cu K}\alpha$ radiation (1.5418 Å) with samples mounted on 25 mm SiO_2 substrates. Data was collected at a 2θ angle range of 3-30 with a step size of 0.04° at 3° per minute, unless otherwise noted.

SCXRD data for $\text{Me}_4\text{L}^{\text{Triaz}}$ was recorded on a Rigaku XtaLAB Mini II diffractometer equipped with a fine-focus sealed X-ray tube ($\text{Mo K}\alpha$ radiation, $\lambda = 0.71073$ Å) at 293 K. The data were integrated and scaled using CrysAlisPro 1.171.40.15 (Rigaku Oxford Diffraction, 2018). An analytical numeric absorption correction using a multifaceted crystal model based on expressions derived by R.C. Clark & J.S. Reid was used.¹ Using Olex2,² the structure was solved with the ShelXT structure solution program³ using Intrinsic Phasing and refined with the SHELXL refinement package using Least Squares minimisation.⁴

SCXRD data for **WUF-52** were collected on a Rigaku Spider diffractometer equipped with a MicroMax MM007 rotating anode generator ($\text{Cu K}\alpha$ radiation, $\lambda = 1.54180$ Å), fitted with high flux Osmic multilayer mirror optics, and a curved image-plate detector. Data were collected at 293 K under d*TREK and were integrated and scaled and averaged with FS-Process.⁵ The crystal structure was solved by direct methods using SHELXS-97 and refined against F^2 on all data by full-matrix least-squares with SHELXL-97.⁶

SCXRD data for **WUF-51** were collected using a Bruker D8 Venture diffractometer equipped with a μS Diamond source ($\text{Cu K}\alpha$ radiation, $\lambda = 1.54180$ Å) and a Photon CPAD detector at 292 K. The data were integrated and scaled and averaged with APEX 3.⁷ SHELXL was used to refine the structure.

¹ Clark, R. C. & Reid, J. S. (1995). *Acta Cryst.* A51, 887-897.

² Dolomanov, O.V., Bourhis, L.J., Gildea, R.J., Howard, J.A.K. & Puschmann, H. (2009). *J. Appl. Cryst.* 42, 339-341.

³ Sheldrick, G.M. (2015). *Acta Cryst.* A71, 3-8.

⁴ Sheldrick, G.M. (2015). *Acta Cryst.* C71, 3-8.

⁵ FSProcess, Rigaku Corporation Tokyo, Japan, 1996.

⁶ Sheldrick, G. M. (1997). SHELXS97 and SHELXL97. University of Göttingen, Germany.

⁷ Bruker (2016). APEX3, SAINT and SADABS. Bruker AXS Inc., Madison, Wisconsin, USA.

Simultaneous TG-DSC data was recorded using a Netzsch STA 449 F3 Jupiter instrument. MOF samples were heated at a rate of 10 °C per min under synthetic air (N₂/O₂ atmosphere (80/20)) at 20 mL/min flow rate for measurements to decomposition, unless noted otherwise.

Gas adsorption studies were carried out using a Quantachrome Autosorb MP instrument and high purity nitrogen (99.999%) gas at the Wollongong Isotope Geochronology Laboratory. Surface areas were determined using Brunauer-Emmett-Teller (BET) calculations.

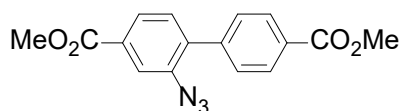
Elemental microanalysis was performed by the Chemical Analysis Facility, Macquarie University, Australia.

2 Synthesis and Spectra of Ligands and Precursors

Synthesis of 2-azido-[1,1'-biphenyl]-4,4'-dicarboxylic acid, H₂bpdcN₃

Me₂bpdcNH₂, Me₂bpdcN₃, and H₂bpdcN₃ were prepared by literature procedures.⁸ Our ¹H NMR spectral data for Me₂bpdcN₃ and H₂bpdcN₃ are shown below.

Dimethyl 2-azido-[1,1'-biphenyl]-4,4'-dicarboxylate, Me₂bpdcN₃



δ_{H} (400 MHz, CDCl₃) 8.13 – 8.09 (2 H, m), 7.94 (1 H, d, *J* 1.5), 7.88 (1 H, dd, *J* 8.0, 1.6), 7.56 – 7.52 (2 H, m), 7.42 (1 H, d, *J* 8.0), 3.97 (3 H, s), 3.95 (3 H, s).

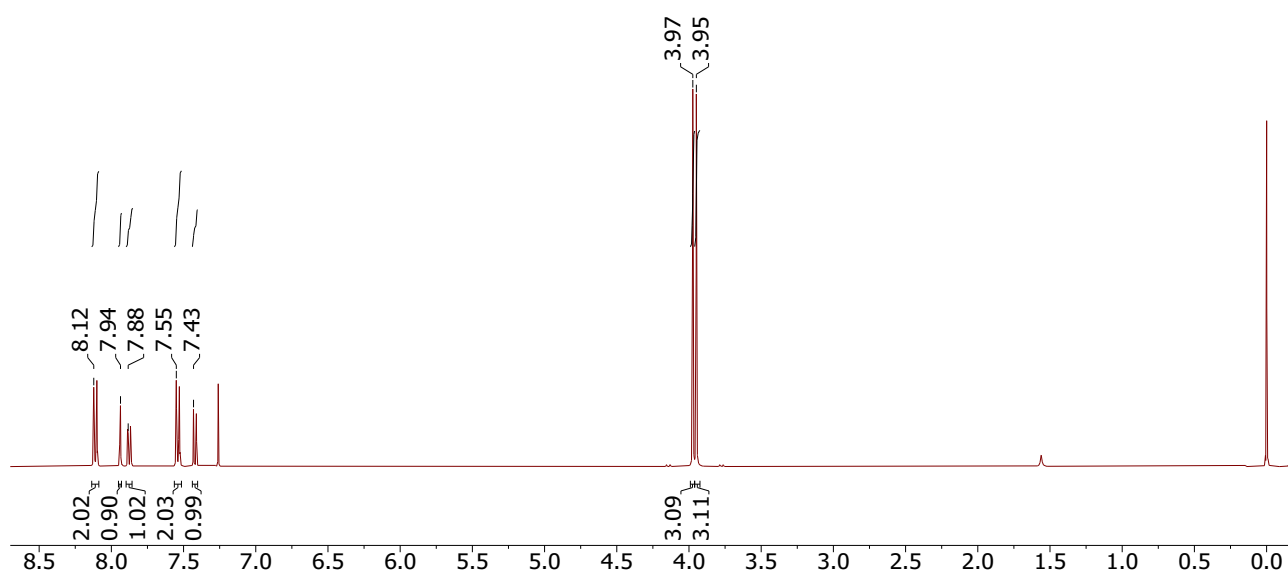
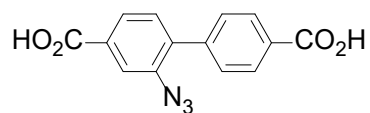


Figure S1: ¹H NMR spectrum for Me₂bpdcN₃ in CDCl₃.

⁸ U. Fluch, B. D. McCarthy and S. Ott, *Dalton Trans.*, 2019, **48**, 45–49.

2-Azido-[1,1'-biphenyl]-4,4'-dicarboxylic acid, H_2bpdCN_3



δ_H (400 MHz, DMSO- d_6) 13.10 (2 H, br s), 8.02 (2 H, d, J 8.2), 7.85–7.81 (2 H, overlapped signals), 7.64 (2 H, d, J 8.2), 7.55 (1 H, d, J 7.9).

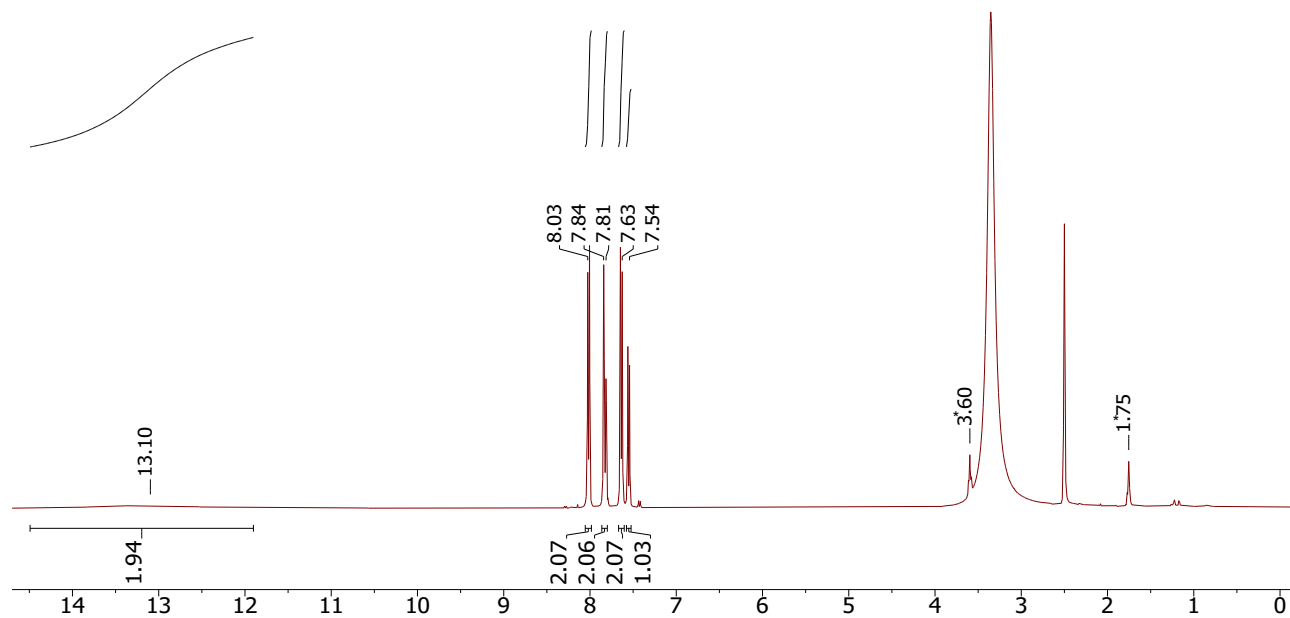
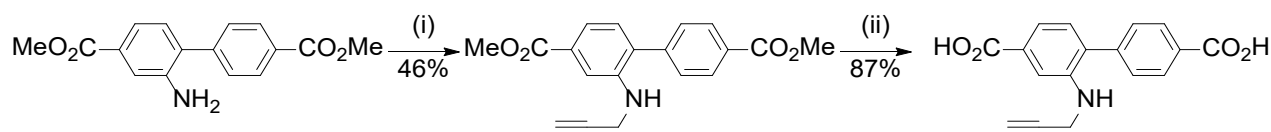


Figure S2: 1H NMR spectrum of H_2bpdCN_3 in DMSO- d_6 . * Signals from residual THF.

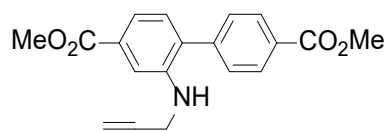
Synthesis of 2-(prop-2-yn-1-ylamino)-[1,1'-biphenyl]-4,4'-dicarboxylic acid, H₂bpdcNHCH₂C≡CH

H₂bpdcNHCH₂C≡CH was synthesised in two steps from Me₂bpdcNH₂, as shown in Scheme S1.



Scheme S1 (i) Propargyl bromide, K₂CO₃, DMF (ii) NaOH_(aq), MeOH/THF.

Dimethyl 2-(prop-2-yn-1-ylamino)-[1,1'-biphenyl]-4,4'-dicarboxylate, Me₂bpdcNHCH₂C≡CH



Propargyl bromide (100 μ L, 0.90 mmol) was added slowly to a stirring suspension of dimethyl 2-amino-[1,1'-biphenyl]-4,4'-dicarboxylate (285.3 mg, 1.01 mmol) and K₂CO₃ (290 mg, 2.10 mmol) in DMF (4.0 mL). The mixture was stirred at 80 °C overnight in a sealed pressure tube. After cooling, the solution was transferred to a conical flask and diluted with H₂O (40 mL) and sonicated for 5 minutes and a precipitate formed. This was collected by vacuum filtration and washed with H₂O (3 \times 10 mL) and air dried. The pale-yellow solid was taken up in EtOAc (80 mL) and washed thrice with H₂O (80 mL) and then with brine (80 mL), dried over MgSO₄ and the solvent removed by rotary evaporation. The residue was purified by column chromatography on silica gel, eluting with 20% petroleum spirit in DCM (R_f = 0.23) and recovered by rotary evaporation of the solvent. Yield 152.0 mg (46%). δ_H (400 MHz, CDCl₃) 8.16 – 8.12 (2 H, m), 7.53 (1 H, dd, J 6.5, 1.2), 7.53 – 7.50 (2 H, m), 7.47 (1 H, d, J 1.6), 7.18 (1 H, d, J 7.8), 4.12 (1 H, t, J 5.8), 3.97 (2 H, dd, J 6.2, 2.6), 3.95 (3 H, s), 3.94 (3 H, s), 2.20 (1 H, t, J 2.4). δ_C (75 MHz, CDCl₃) 167.32, 166.82, 143.80, 143.08, 131.73, 130.95, 130.45, 130.28, 129.73, 129.31, 119.70, 112.29, 80.40, 71.81, 52.41, 52.33, 33.68.

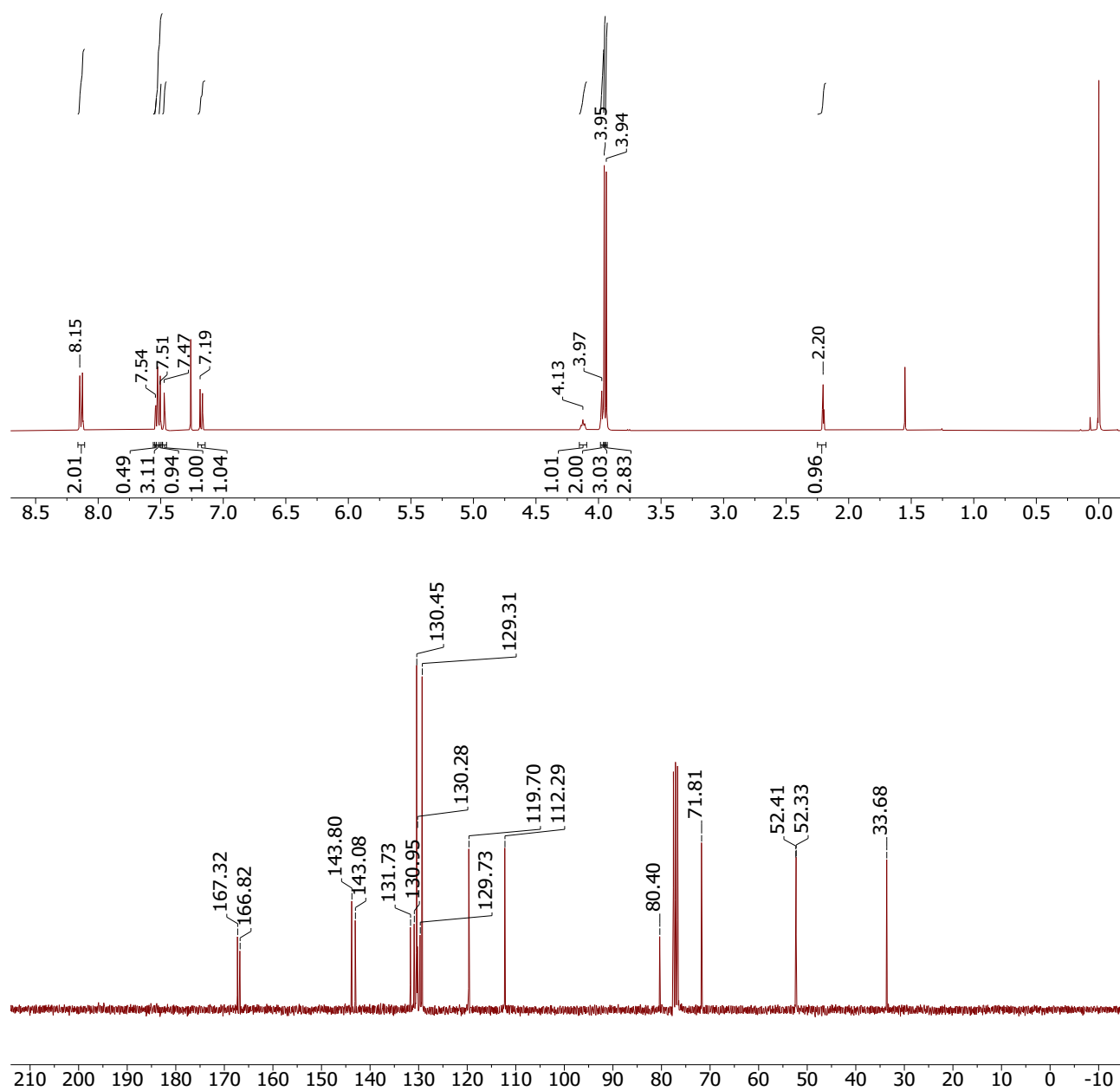
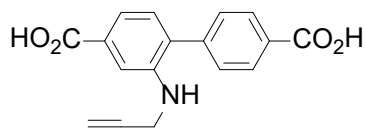


Figure S3: ¹H NMR spectrum (top) and ¹³C NMR spectrum (bottom) of Me₂bpdCNHCH₂C≡CH in CDCl₃.

2-(Prop-2-yn-1-ylamino)-[1,1'-biphenyl]-4,4'-dicarboxylic acid, $H_2bpdCNHCH_2C\equiv CH$



1 M aqueous NaOH (975 μ L, 0.975 mmol) was added drop wise to a stirring solution of dimethyl 2-(prop-2-yn-1-ylamino)-[1,1'-biphenyl]-4,4'-dicarboxylate (150.0 mg, 0.464 mmol) dissolved in a mixture of THF (975 μ L) and MeOH (975 μ L), and stirring was continued overnight. The THF and MeOH were removed via rotary evaporation and H₂O (8 mL) was added and then the pH adjusted to 3 using 1 M HCl. The precipitate that developed was collected via vacuum filtration, washed with H₂O (2 \times 10 mL) and dried in air. Yield 119.9 mg (87%). δ_H (400 MHz, DMSO- d_6) 12.91 (2 H, s), 8.06 – 8.01 (2 H, m), 7.55 – 7.50 (2 H, m), 7.40 (1 H, d, J 1.6), 7.34 (1 H, dd, J 7.7, 1.6), 7.15 (1 H, d, J 7.8), 5.45 (1 H, t, J 6.0), 3.90 (2 H, dd, J 6.1, 2.5), 3.06 (1 H, t, J 2.3). δ_C (101 MHz, DMSO- d_6) δ 167.63, 167.16, 144.25, 142.82, 131.21, 130.58, 130.23, 129.92, 129.89, 129.16, 118.19, 112.04, 81.87, 73.16, 32.40.

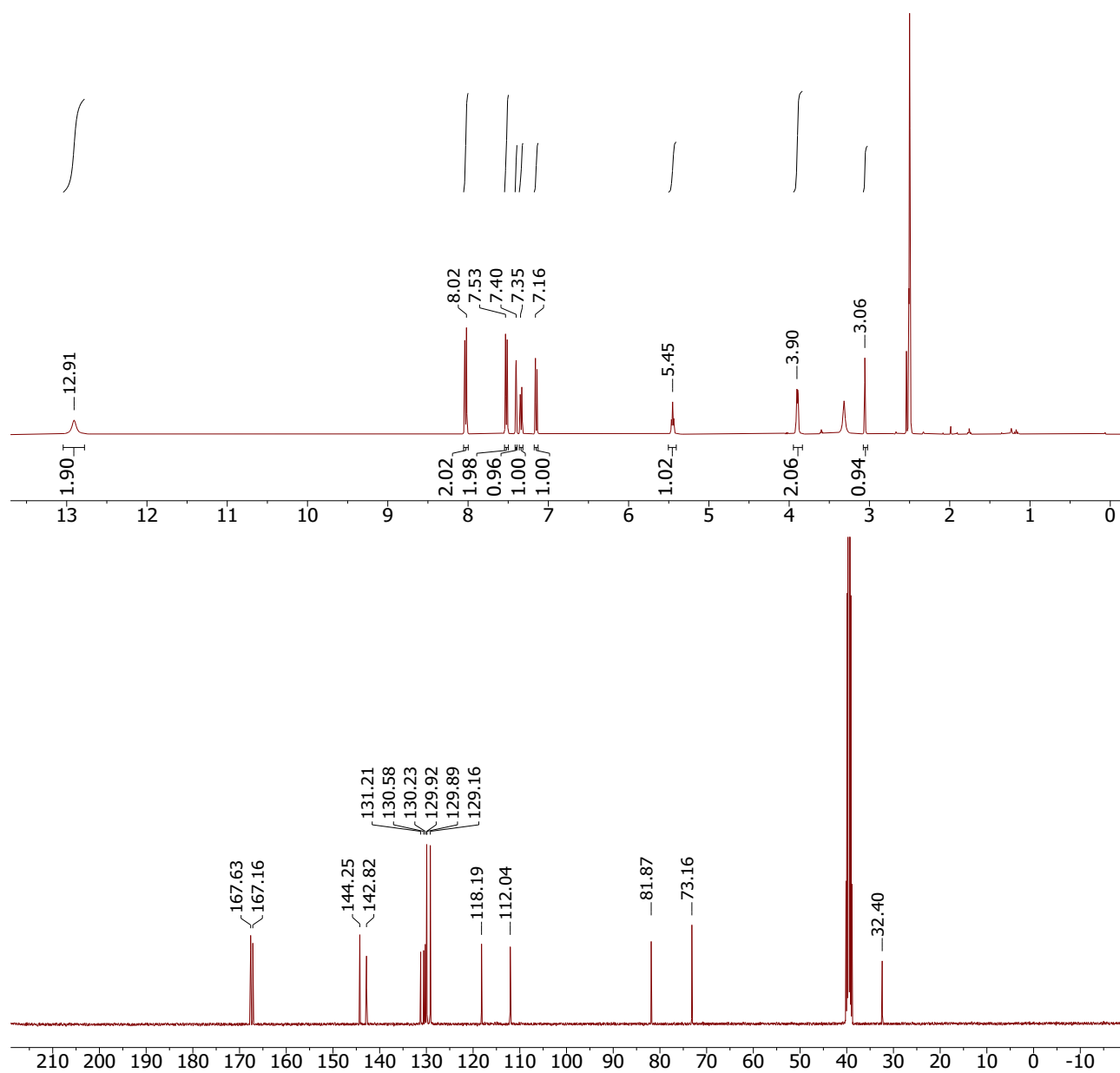
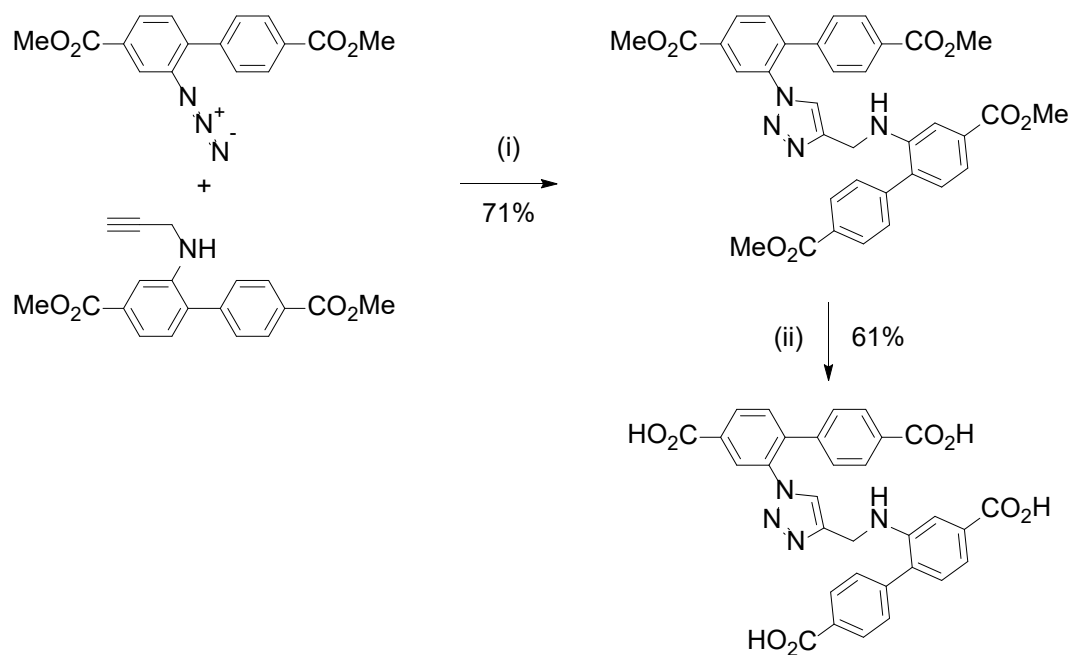


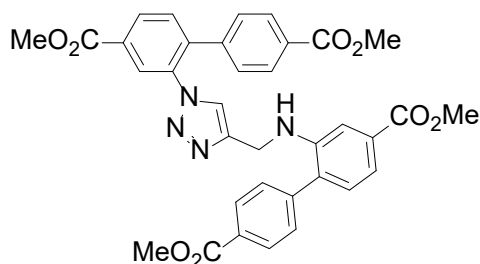
Figure S4: ¹H NMR spectrum (top) and ¹³C NMR spectrum (bottom) of H₂bpdCNHCH₂C≡CH in DMSO-*d*₆.

Synthesis of 2-(((1-(4,4'-dicarboxy-[1,1'-biphenyl]-2-yl)-1H-1,2,3-triazol-4-yl)methyl)amino)-[1,1'-biphenyl]-4,4'-dicarboxylic acid, 1,4- H_4L^{Triaz}



Scheme S2 i) CuSO_4 , sodium ascorbate, DMF/ H_2O , (ii) $\text{NaOH}_{(\text{aq})}$, MeOH/THF.

Dimethyl 2-(((1-(4,4'-bis(methoxycarbonyl)-[1,1'-biphenyl]-2-yl)-1H-1,2,3-triazol-4-yl)methyl)amino)-[1,1'-biphenyl]-4,4'-dicarboxylate, 1,4-Me₄L^{Triaz}



Me₂bpdCN₃ (37.5 mg, 0.12 mmol) and Me₂bpdCNHCH₂C≡CH (35.5 mg, 0.11 mmol) were dissolved in a solution of 3:1 DMF/H₂O (8 mL) in a sealable glass tube. Sodium ascorbate (21.8 mg, 0.11 mmol) and CuSO₄·5H₂O (14.7 mg, 0.059 mmol) were added and the solution was stirred overnight at 50 °C. The mixture was diluted with H₂O (60 mL) and thrice extracted with EtOAc (60 mL). The organic phase was washed with H₂O (3 × 50 mL), brine (50 mL), and dried over Na₂SO₄ and the solvent was removed completely by rotary evaporation. The solid was taken up in DCM and passed through a plug of silica gel eluting with DCM, followed by 5% EtOAc in DCM to collect the product. Yield 51.5 mg (71%). δ_H (500 MHz, CDCl₃) 8.28 (1 H, d, *J* 1.6), 8.24 (1 H, dd, *J* 8.1, 1.7), 8.13 – 8.10 (2 H, m), 7.86 – 7.83 (2 H, m), 7.58 (1 H, d, *J* 8.1), 7.45 – 7.42 (1 H, m), 7.45 – 7.42 (2 H, m), 7.30 (1 H, d, *J* 1.6), 7.20 (1 H, s), 7.12 (1 H, d, *J* 7.8), 7.12 – 7.06 (2 H, m), 4.46 (1 H, t, *J* 5.9), 4.40 (2 H, d, *J* 5.8), 3.97 (3 H, s), 3.95 (3 H, s), 3.91 (3 H, s), 3.90 (3 H, s). δ_C (101 MHz, CDCl₃) 167.28, 166.83, 166.36, 165.50, 145.49, 143.99, 143.12, 140.93, 140.54, 135.14, 131.48, 131.44, 131.35, 131.09, 130.83, 130.53, 130.40, 130.35, 130.04, 129.80, 129.18, 128.38, 128.13, 123.78, 119.22, 111.63, 52.78, 52.38, 52.36, 52.29, 39.27.

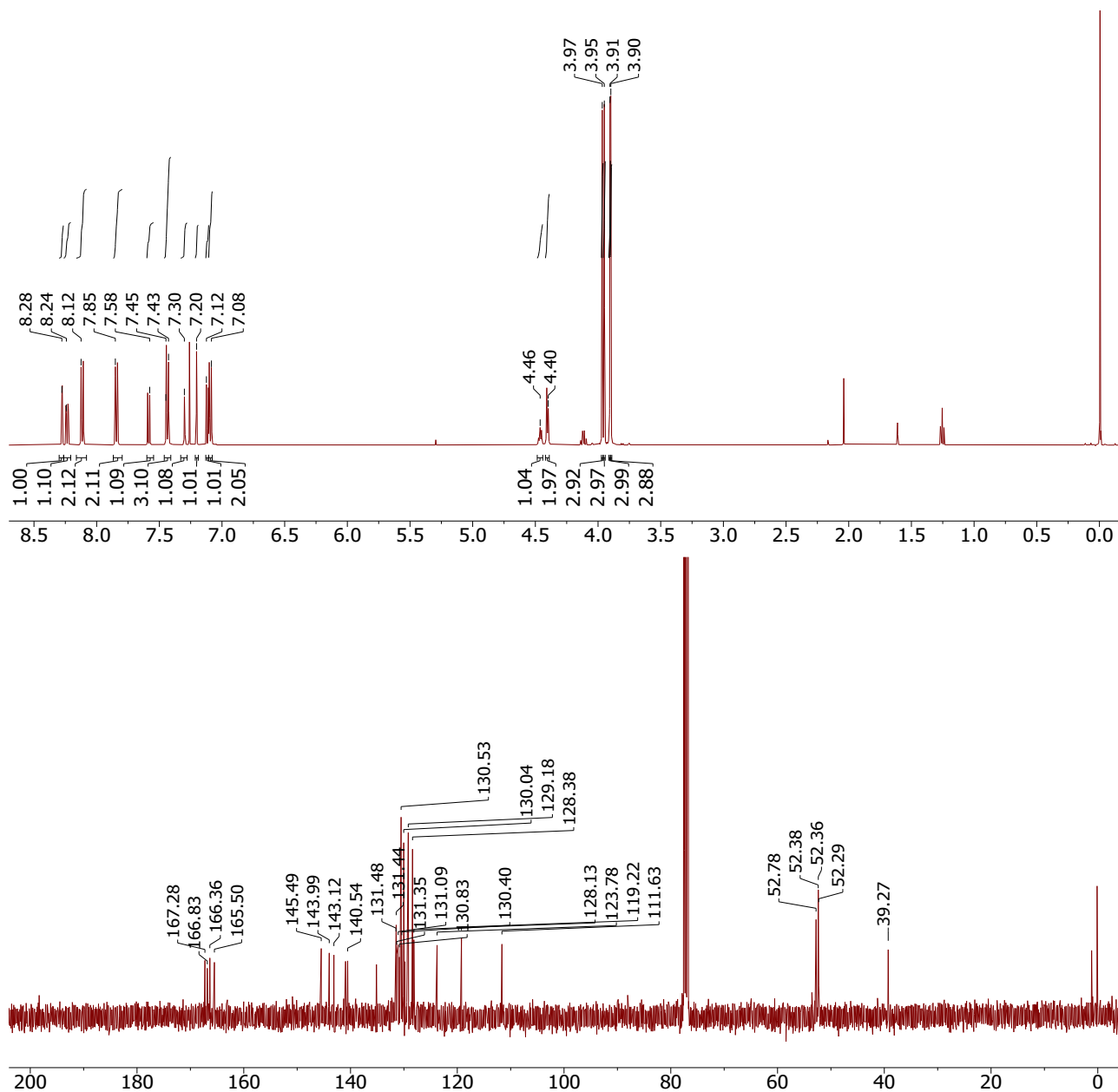
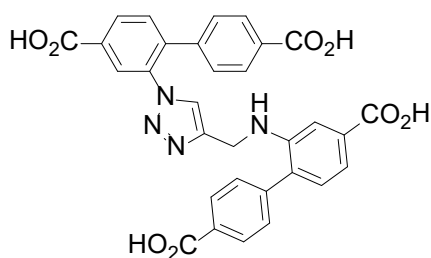


Figure S5: ¹H NMR spectrum (top) and ¹³C NMR spectrum (bottom) of 1,4-Me₄L^{Triaz} in CDCl₃.

2-(((1-(4,4'-dicarboxy-[1,1'-biphenyl]-2-yl)-1H-1,2,3-triazol-4-yl)methyl)amino)-[1,1'-biphenyl]-4,4'-dicarboxylic acid, 1,4- H_4L^{Triaz}



1,4- Me_4L^{Triaz} (47.7 mg, 0.08 mmol) was dissolved in a 1-1 solution of MeOH-THF (2 mL) and 1 M NaOH (0.5 mL, 0.5 mmol) was added the mixture was stirred for 2 days. The organic solvent was reduced in volume by rotary evaporation and the solution was acidified with 1 M HCl until pH 2. A yellow solid precipitated and this was filtered and washed with water (2×5 mL). Yield 26.3 mg (61%). δ_H (400 MHz, DMSO- d_6) 13.00 (4 H, s), 8.19 (1 H, dd, J 8.0, 1.8), 8.04 (2 H, d, J 8.6), 8.02 (2 H, d, J 8.0), 7.75 (1 H, d, J 7.9), 7.74 (2 H, d, J 8.3), 7.51 (2 H, d, J 8.3), 7.32 – 7.26 (1 H, m), 7.28 (1 H, s), 7.11 (2 H, d, J 8.3), 7.10 (1 H, d, J 8.2), 5.52 (1 H, t, J 5.9), 4.37 (2 H, d, J 5.6). δ_C (101 MHz, DMSO- d_6) 167.57, 167.10, 166.76, 165.90, 145.98, 144.37, 143.00, 140.72, 140.08, 134.76, 131.74, 131.59, 131.16, 130.64, 130.39, 130.23, 130.15, 129.88, 129.77, 129.37, 129.10, 128.17, 127.24, 124.89, 117.84, 111.44, 38.47.

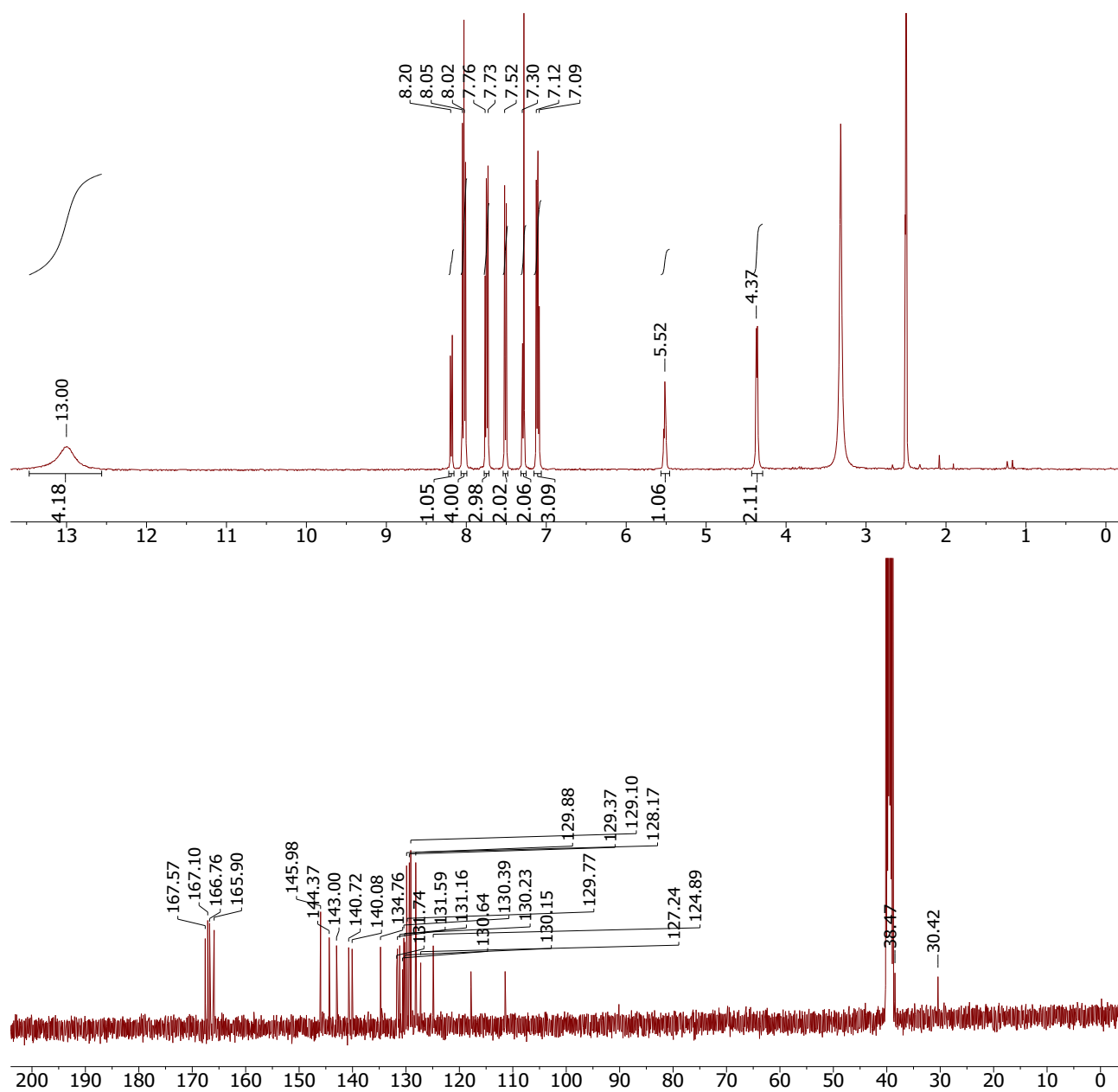
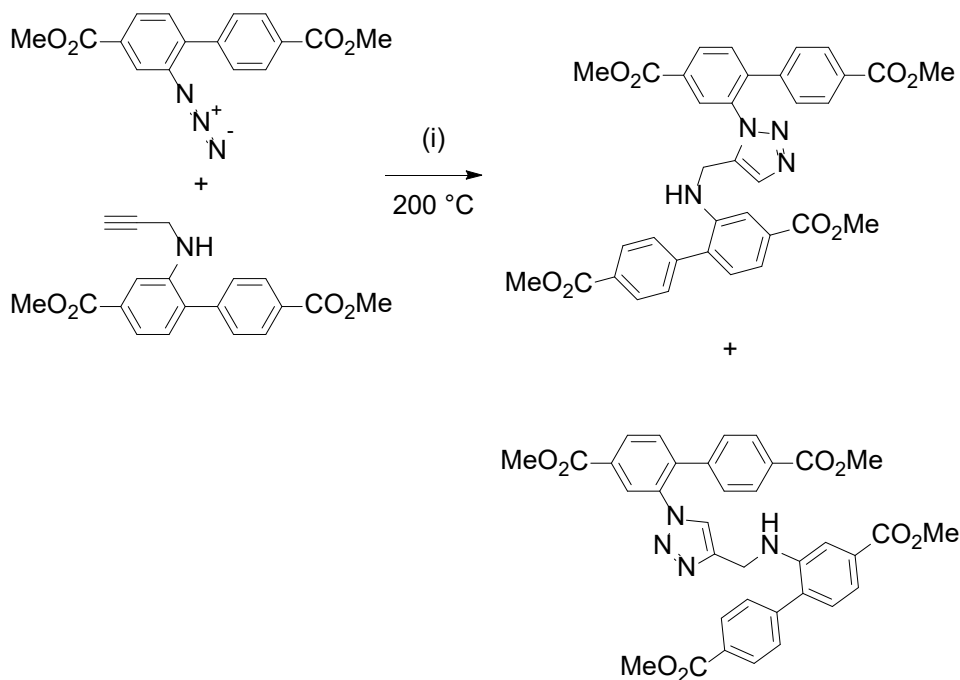


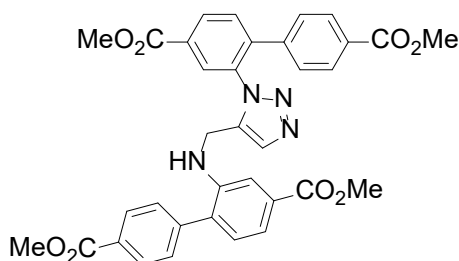
Figure S6: ¹H NMR spectrum (top) and ¹³C NMR spectrum (bottom) of 1,4-H₄L^{Triaz} in DMSO-*d*₆.

Synthesis of dimethyl 2-(((1-(4,4'-bis(methoxycarbonyl)-[1,1'-biphenyl]-2-yl)-1H-1,2,3-triazol-5-yl)methyl)amino)-[1,1'-biphenyl]-4,4'-dicarboxylate, 1,5-Me₄L^{Triaz}



Scheme S3

Dimethyl 2-(((1-(4,4'-bis(methoxycarbonyl)-[1,1'-biphenyl]-2-yl)-1H-1,2,3-triazol-5-yl)methyl)amino)-[1,1'-biphenyl]-4,4'-dicarboxylate, 1,5-Me₄L^{Triaz}



1,5-Me₄L^{Triaz} was synthesized on a 5 mg scale as a mixture of regioisomers by directly heating a pre-ground equimolar mixture of Me₂bpdCN₃ and Me₂bpdCNHCH₂C≡CH under N₂ atmosphere to 200 °C at 10 °C per minute in a TG-DSC analyser. After cooling the solid was dissolved in CDCl₃ for analysis by ¹H NMR spectroscopy.

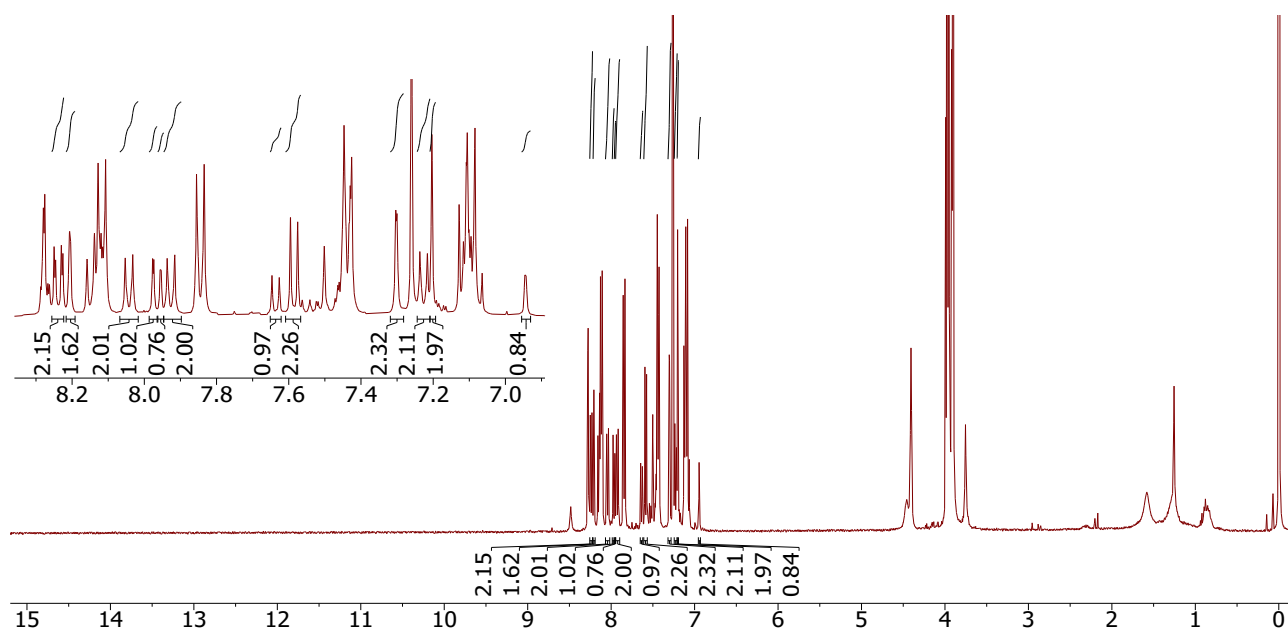


Figure S7: ^1H NMR spectrum of the crude reaction mixture containing an $\sim 2.2:1$ mixture of 1,4- $\text{Me}_4\text{L}^{\text{Triaz}}$ and 1,5- $\text{Me}_4\text{L}^{\text{Triaz}}$, respectively, in CDCl_3 .

3 Synthesis of Metal-organic Frameworks

General solvent exchange procedure

Crystals were transferred into a clean vial immediately following removal from the oven. The reaction solvent was pipetted away and replaced by fresh anhydrous DMF (2 mL). This was repeated twice more with two-hour intervals between exchanges. The crystals were changed from DMF to acetone, then to DCM, then to cyclohexane by the same process as above with exchanges, ~every two hours.

Activation procedure

The samples, in the minimum of frozen cyclohexane solvent, were activated by freeze drying at -53°C and 0.09 mbar for 1 hour followed by heating under dynamic vacuum at 100°C for **WUF-50**, **WUF-51** and **WUF-53** and 120°C for **WUF-52** for 6 hours each.

$Zn_4O(bpdcN_3)_{0.63}(bpdcNHCH_2C\equiv CH)_{0.59}(tria)_{0.89} [Zn_4O(L^1)_{0.63}(L^2)_{0.59}(L^{Triaz})_{0.89}]$ (**WUF-50**)

To anhydrous DMF (8.0 mL) was added $Zn(NO_3)_2 \cdot 6H_2O$ (170.0 mg, 0.571 mmol), H_2bpdcN_3 (30.0 mg, 0.106 mmol) and $H_2bpdcNHCH_2C\equiv CH$ (35.5 mg, 0.120 mmol) and the mixture was sonicated until homogeneous and split into two vials (4.0 mL each). The solutions were heated at 100 °C for 18 hours and the light brown crystals were transferred to a clean vial and washed with anhydrous DMF. Yield: 39.8 mg (50%). Anal. Calc. for $C_{46.5}H_{43}N_6O_{21}Zn_4 \cdot [Zn_4O(bpdcN_3)_{0.63}(bpdcNHCH_2C\equiv CH)_{0.59}(L^{Triaz})_{0.89}] \cdot 7H_2O$: C, 44.09; H, 3.26; N, 6.69. Found: C, 43.90; H, 3.23; N, 6.44.

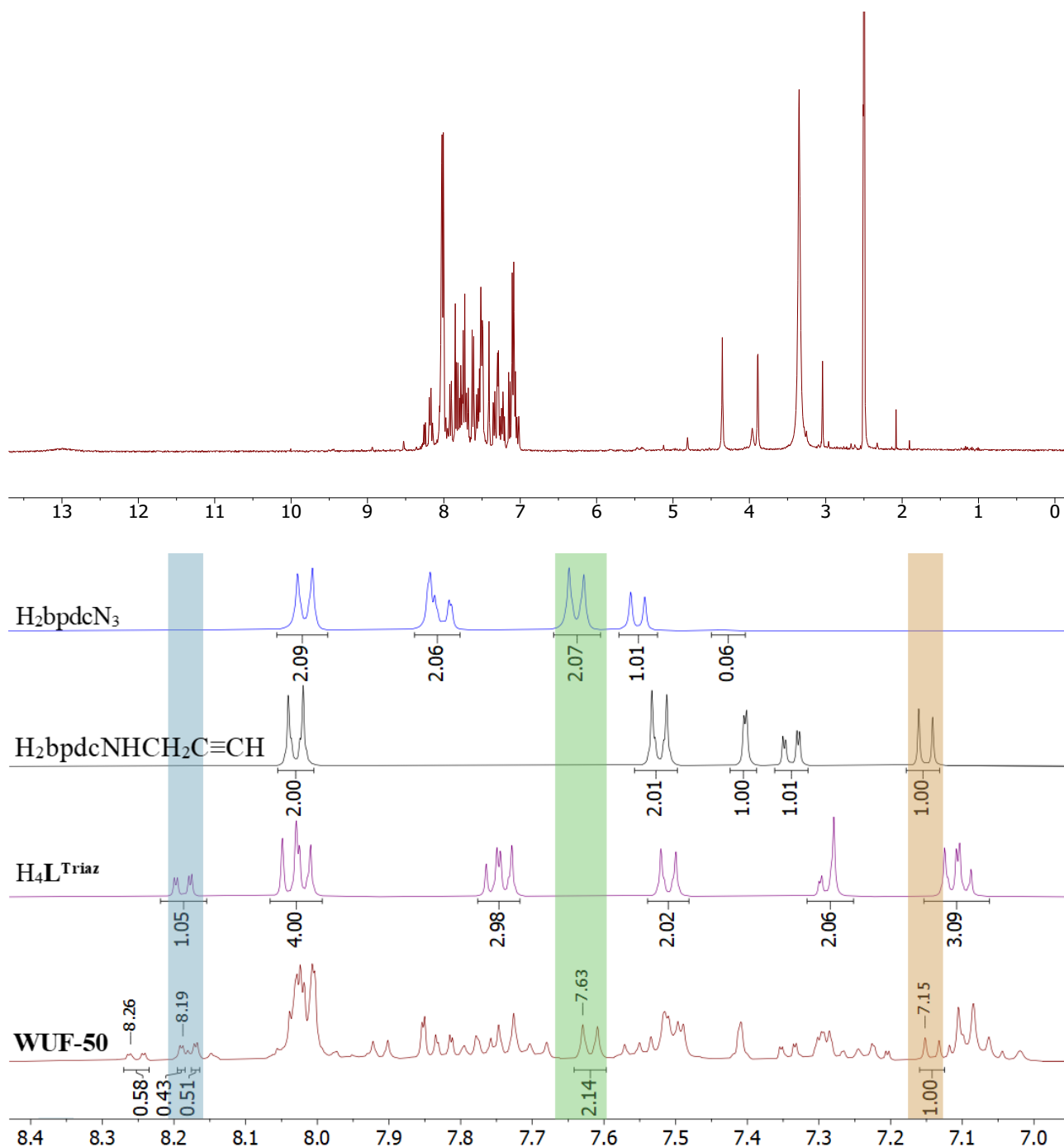


Figure S8: 1H NMR spectrum of **WUF-50** digested in $DCl / DMSO-d_6$ (top). Stacked 1H NMR spectra of **WUF-50** and molecular components (bottom).

Zn₄O(bpdcN₃)₃ (WUF-51)

To anhydrous DMF (8.0 mL) was added Zn(NO₃)₂·6H₂O (120.1 mg, 0.40 mmol) and H₂bpdcN₃ (60.0 mg, 0.21 mmol) and the mixture was sonicated until homogeneous and split into two vials (4.0 mL each). The solutions were heated at 100 °C for 18 hours and the pale-yellow crystals were transferred to a clean vial and washed with anhydrous DMF. Yield 36.4 mg (46%). Anal. Calcd for C₄₂H₂₅N_{8.9}O₁₅Zn₄ | [Zn₄O(bpdcN₃)_{2.94}(2,7-cdc)_{0.06}·2H₂O]*: C, 43.65; H, 2.18; N, 10.76. Found: C, 43.90; H, 2.03; N, 10.07.

* Crystals from the synthesis contain only around 2% 9*H*-carbazole-2,7-dicarboxylate (cdc). Samples sent for elemental analysis were dried by the service provider at 120 °C overnight and then left to cool in the air before analysis. When we repeated this process, we saw 2% conversion to the carbazole (¹H NMR spectrum below) and our analysis figures reflect this composition.

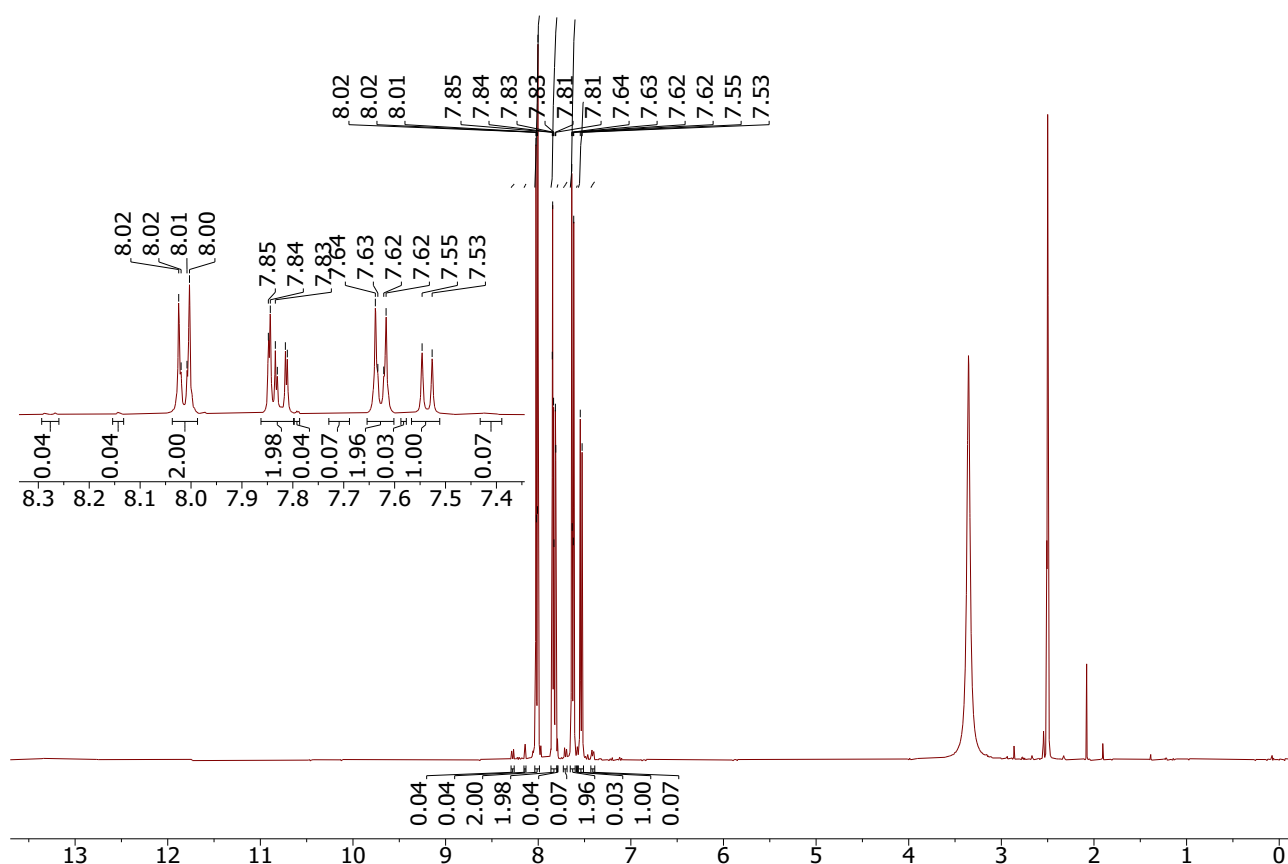


Figure S9: ¹H NMR spectrum of **WUF-51** digested in DCl / DMSO-*d*₆.

Zn₄O(bpdCNHCH₂C≡CH)₃ (WUF-52)

To anhydrous DMF (4.0 mL) was added H₂bpdCNHCH₂C≡CH (31.0 mg, 0.10 mmol) and Zn(NO₃)₂·6H₂O (59.6 mg, 0.20 mmol) and the mixture was sonicated until homogeneous. The solution was heated at 100 °C for 18 hours and the resulting crystals were transferred to a clean vial and washed with anhydrous DMF then anhydrous DCM before digestion in DCl and DMSO-*d*₆ for ¹H NMR analysis.

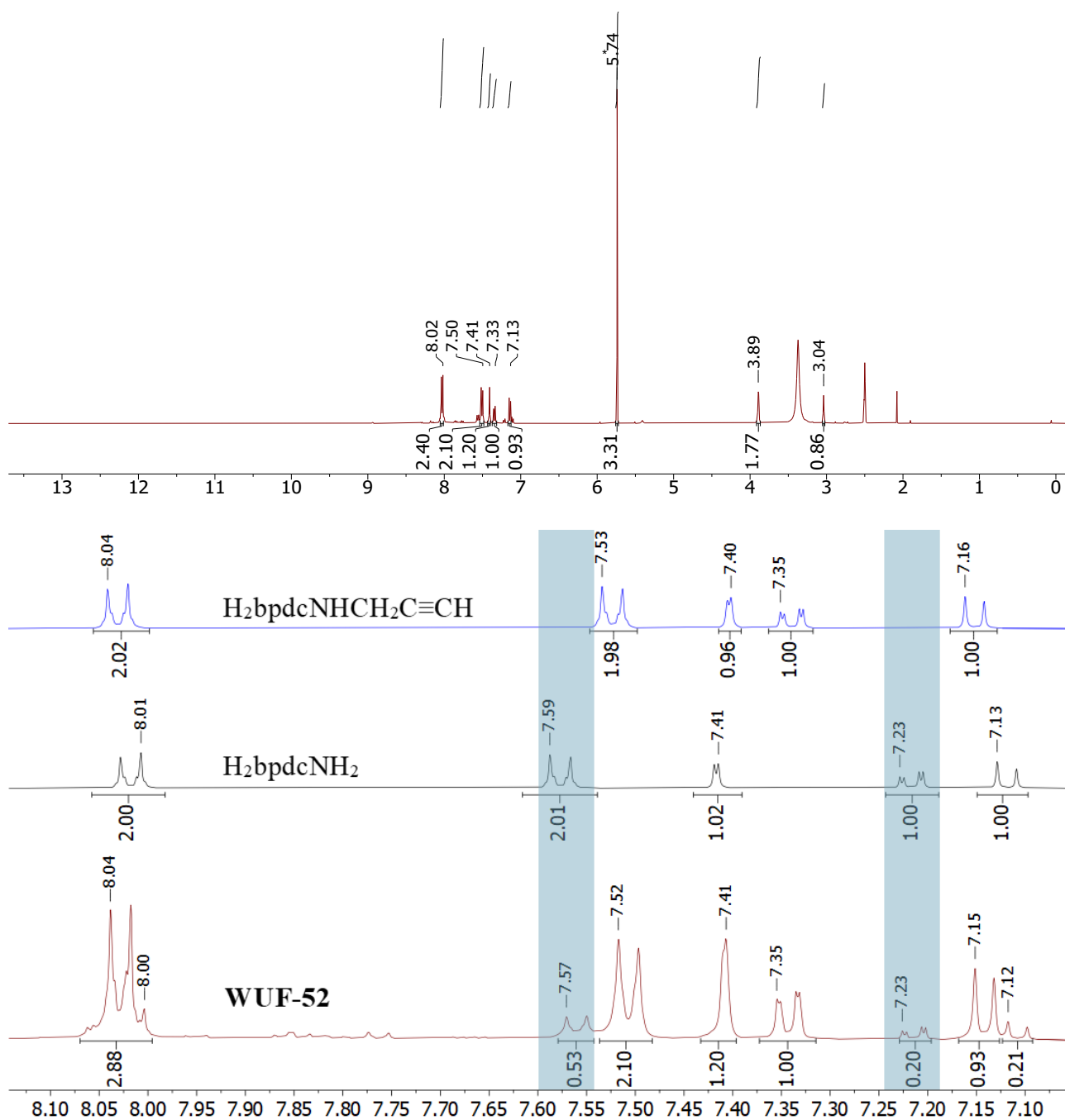


Figure S10: ¹H NMR spectrum (top) of **WUF-52** digested in DCl / DMSO-*d*₆. Stacked ¹H NMR spectra of digested **WUF-52** and molecular components (bottom). * indicates residual DCM.

$\text{Zn}_4\text{O}(\text{bpdc-NH}_2)_{0.60}(\text{1,4-L}^{\text{Triaz}})_{1.20}$ (WUF-53)

To anhydrous DMF (20.0 mL) was added $\text{Zn}(\text{NO}_3)_2 \cdot 6\text{H}_2\text{O}$ (406.5 mg, 1.36 mmol) and 1,4- $\text{H}_4\text{L}^{\text{Triaz}}$ (152.0 mg, 0.26 mmol) and the mixture was sonicated until homogeneous and split into five reaction vials. After heating the solution at 100 °C for 18 hours a white precipitate was observed in the bottom of the reaction vials. After 36 hours of heating, crystals had formed amongst the precipitate and these were separated and transferred to a clean vial and washed with anhydrous DMF and then anhydrous DCM before some vacuum drying and digestion for analysis by ^1H NMR spectroscopy.

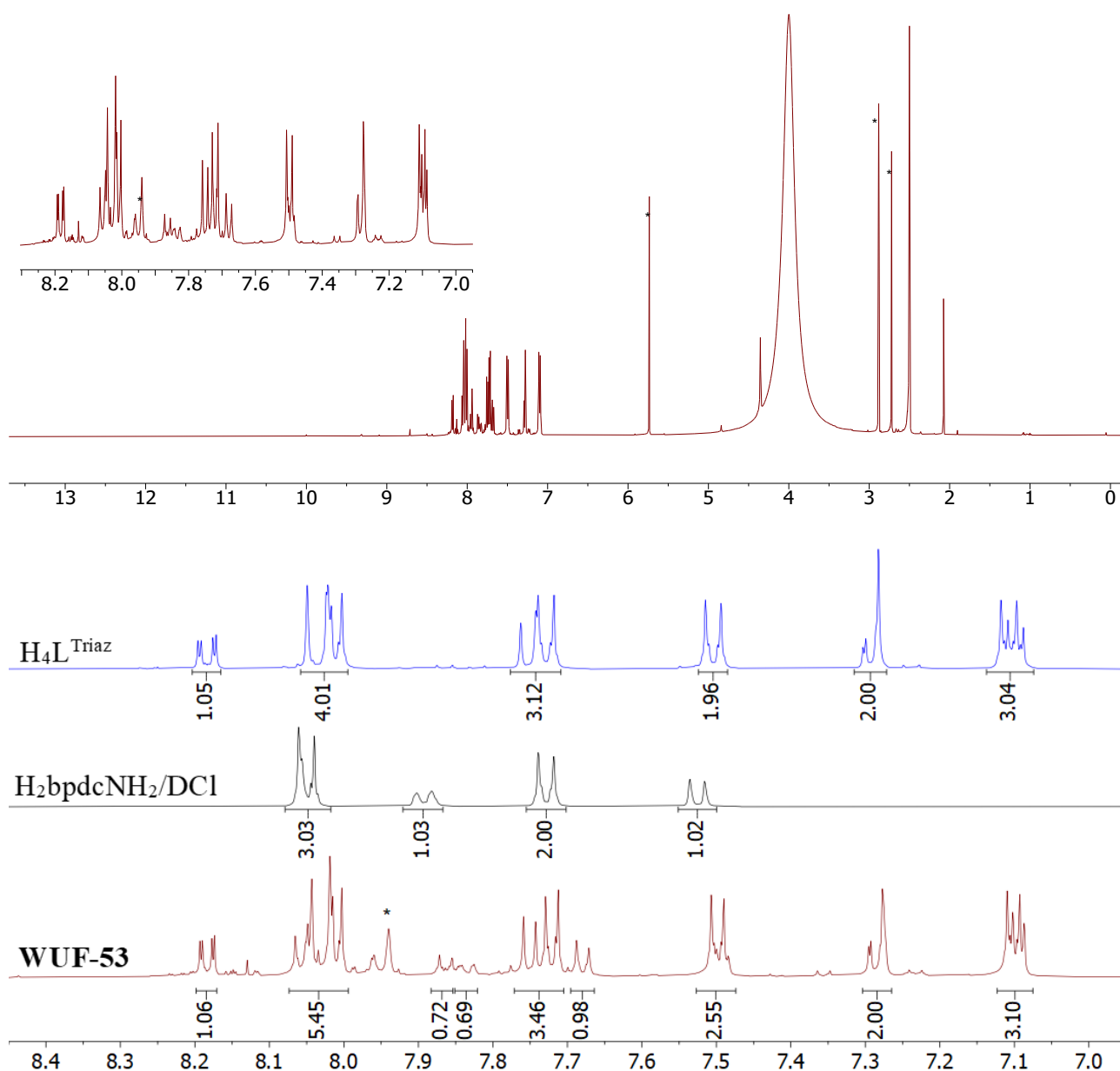


Figure S11: ^1H NMR spectrum (top) of $\text{Zn}_4\text{O}(\text{bpdc-NH}_2)_{0.60}(\text{L}^{\text{Triaz}})_{1.20}$ digested in DCl and $\text{DMSO-}d_6$. Stacked ^1H NMR spectra (bottom) in DCl / $\text{DMSO-}d_6$ of $\text{H}_4\text{L}^{\text{Triaz}}$ (blue), $\text{H}_2\text{bpdcNH}_2$ (black) and digested **WUF-53** (maroon). * indicates residual DMF and DCM that were not removed during vacuum drying.

$Zn_4O(cdc)_3$ (PS-WUF-54) (*cdc*=9H-carbazole-2,7-dicarboxylate)

Activated crystals of pale yellow **WUF-51** were heated under vacuum at 220 °C for 45 minutes to produce darker, brown crystals of PS-**WUF-54**. These were immediately analyzed by gas adsorption and then digested in DCl and DMSO- d_6 for analysis by 1H NMR spectroscopy.

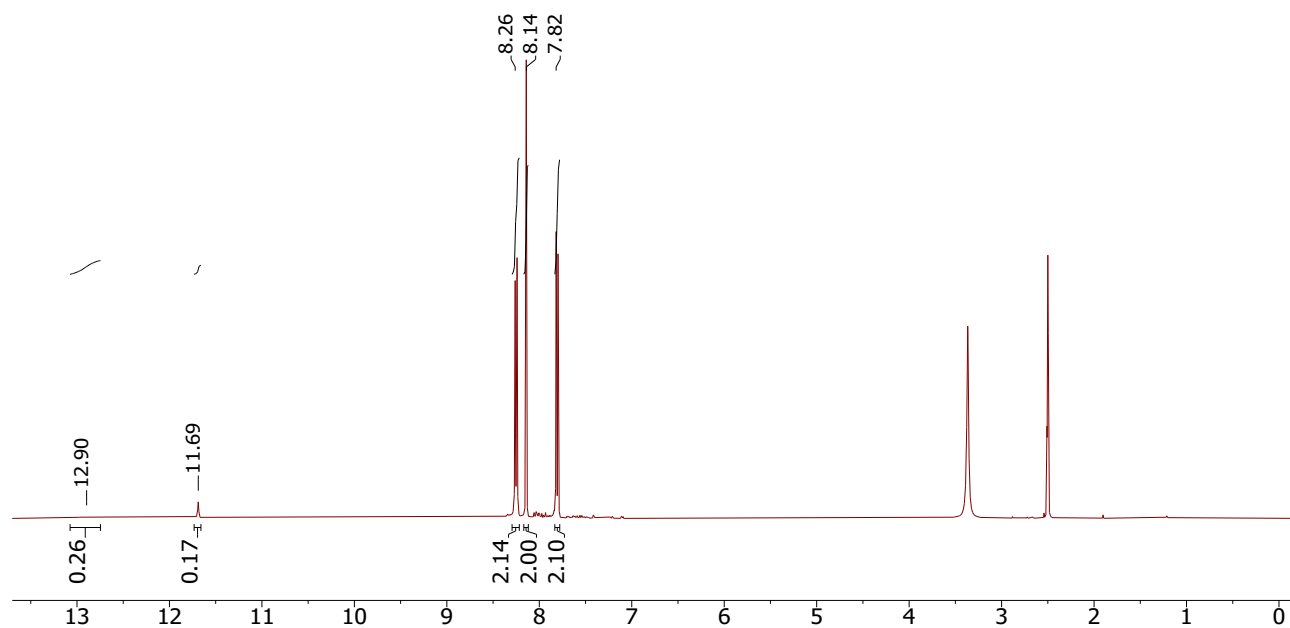


Figure S12: 1H NMR spectrum of PS-**WUF-54** digested in DCl / DMSO- d_6 .

4 Control Reactions

Control reaction of Me₂bpdCN₃ and Me₂bpdCNHCH₂C≡CH under MOF forming conditions

Me₂bpdCN₃ (10.0 mg, 0.0321 mmol) and Me₂bpdCNHCH₂C≡CH (10.3 mg, 0.0319 mmol) were dissolved in DMF (2.0 mL) along with Zn(NO₃)₂·6H₂O (37.5 mg, 0.13 mmol) and heated at 100 °C for 16 hours. The reaction was cooled and the DMF removed under vacuum. Recovered 14.9 mg (73 %).

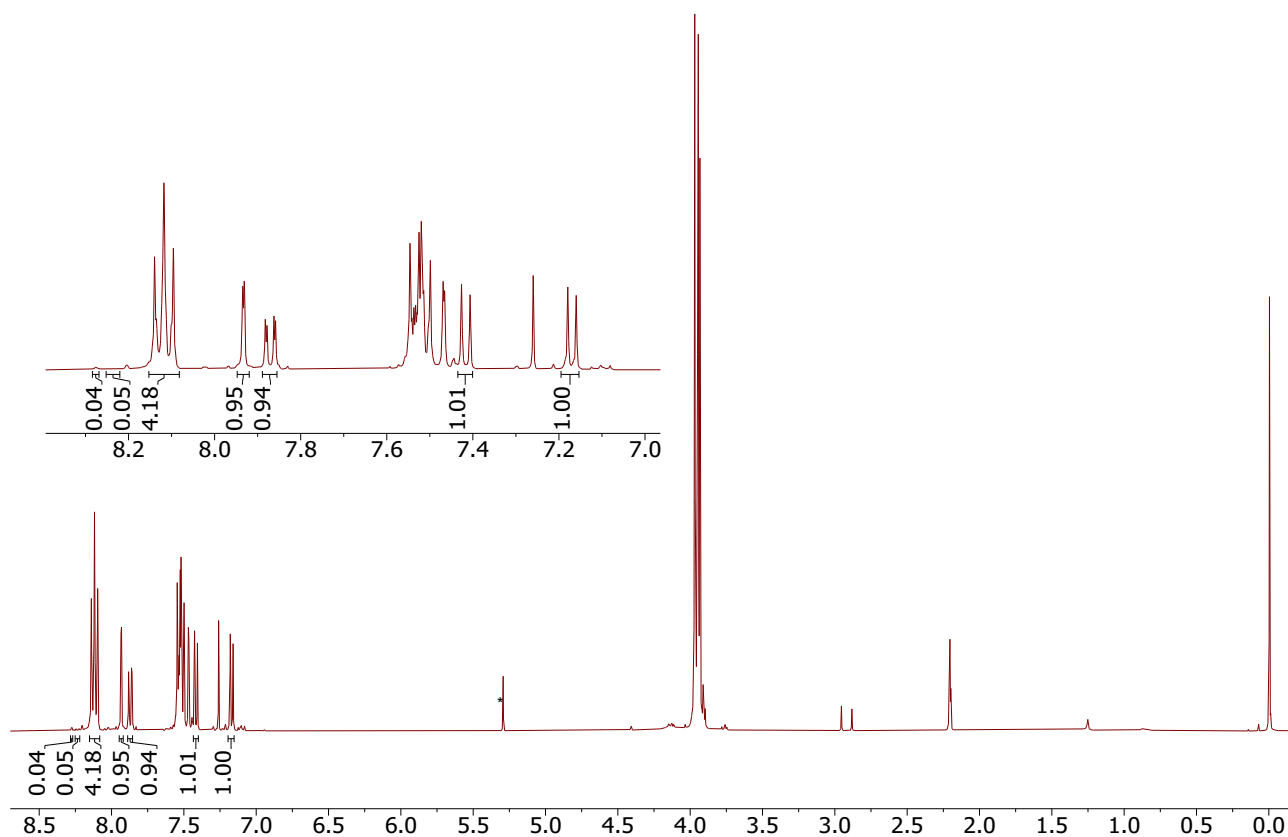


Figure S13: ¹H NMR spectrum in CDCl₃ of material recovered from the control reaction of Me₂L¹ and Me₂L². Signals representing Me₄L^{Triaz} formation are 2%. * indicates residual DCM.

Control reaction of Me₄L^{Triaz} under MOF-forming conditions

Me₄L^{Triaz} (33.6 mg, 0.053 mmol) and Zn(NO₃)₂·6H₂O (78.1 mg, 0.26 mmol) were dissolved in DMF (4.0 mL) and heated at 100 °C for 36 hours. The reaction was cooled and the DMF was removed under vacuum. The solid was suspended in H₂O and the aqueous phase was extracted with EtOAc (3 × 20 mL). The organic phase was washed with H₂O (3 × 20 mL) and brine (20 mL) and dried over Na₂SO₄ and the solvent removed. The yellow solid was dissolved in acetone and filtered through a Celite plug and dried under vacuum. Recovered 37.4 mg.

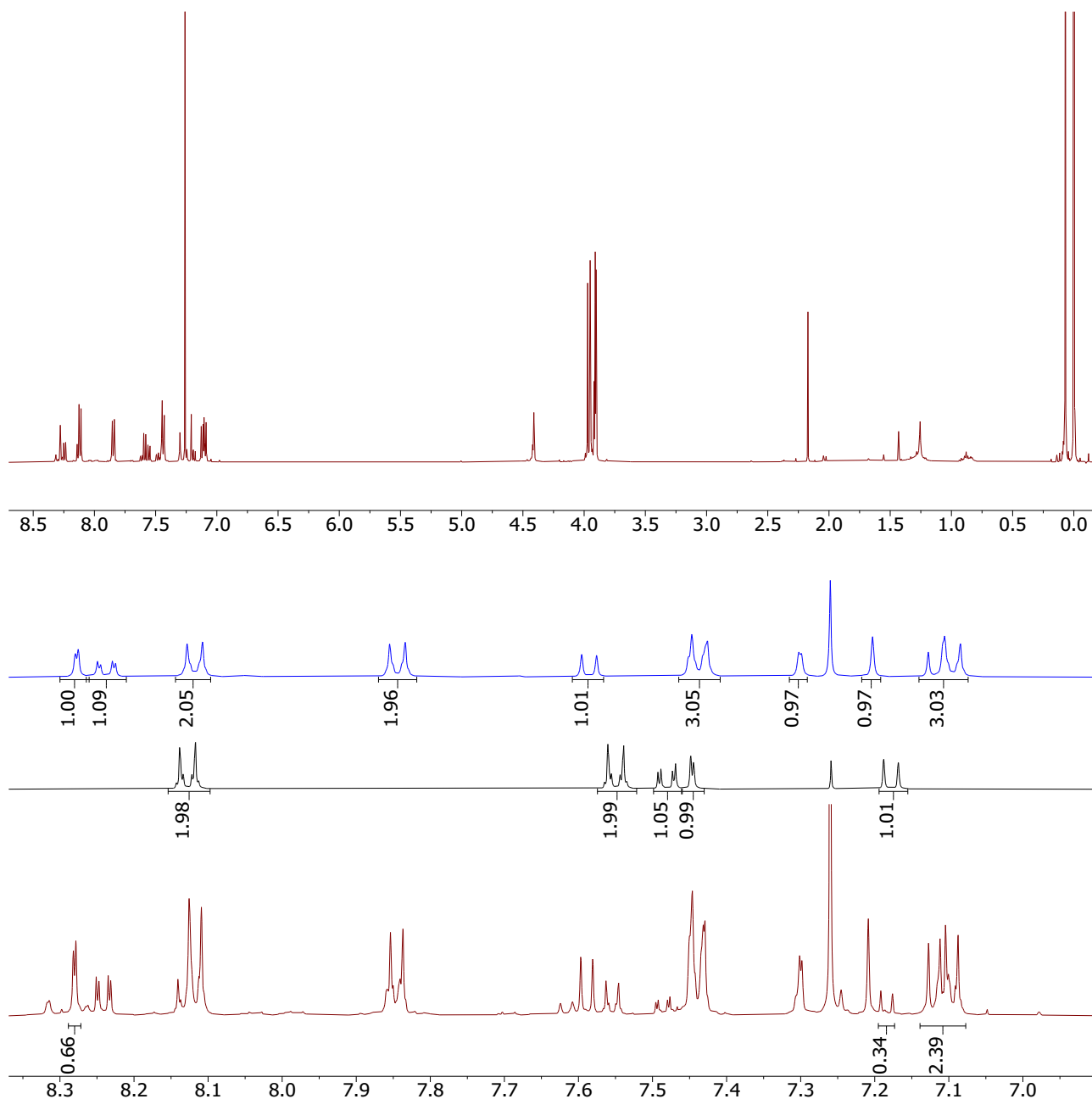


Figure S14: ¹H NMR spectrum (top) in CDCl₃ of recovered material from the control reaction (Me₄L^{Triaz} to 34% Me₂bpdcNH₂). Stacked ¹H NMR spectra (bottom) in CDCl₃ of Me₄L^{Triaz} (blue), Me₂bpdcNH₂ (black) and the material recovered from the control reaction (maroon).

Control reaction of Me₂L² under MOF-forming conditions

Me₂L² (32.0 mg, 0.10 mmol) and Zn(NO₃)₂·6H₂O (94.0 mg, 0.32 mmol) were dissolved in DMF (9.0 mL) and heated at 100 °C for 24 hours. The reaction was cooled and most of the DMF was removed under vacuum. The residue was diluted with H₂O (15 mL) and the solid was collected by filtration and washed with H₂O (3 × 2 mL) and oven dried. Recovered 28.7 mg. ¹H NMR spectroscopy showed no C-N bond cleavage.

5 Powder X-ray Diffraction

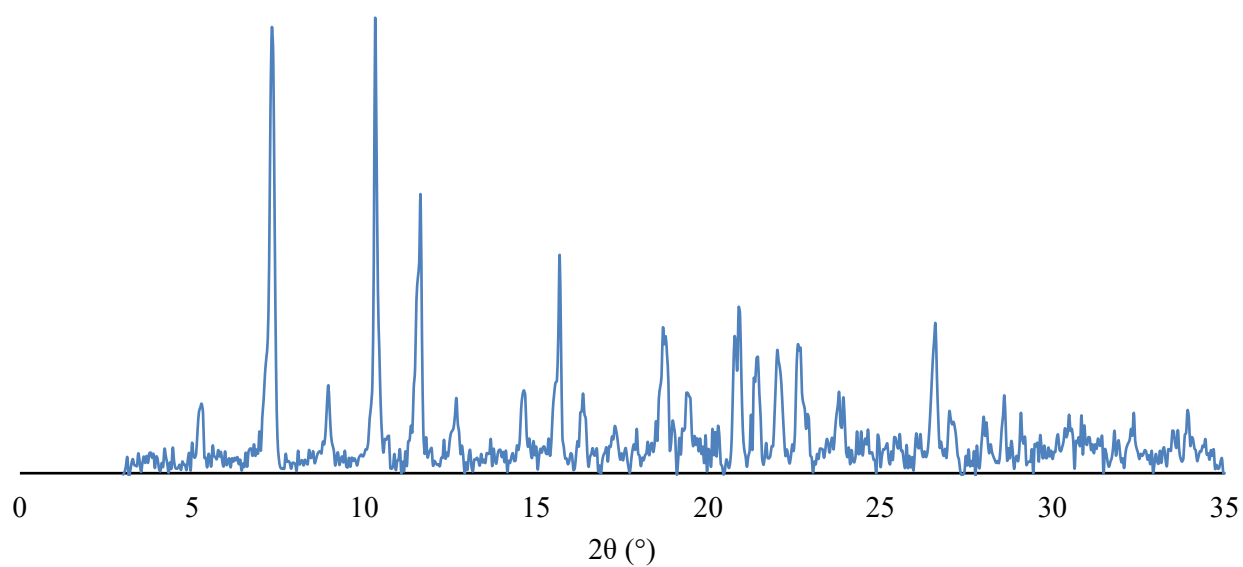


Figure S15: Experimental PXRD trace of as-synthesised **WUF-50**. 3-35°, 0.04 step size, 2°/min.

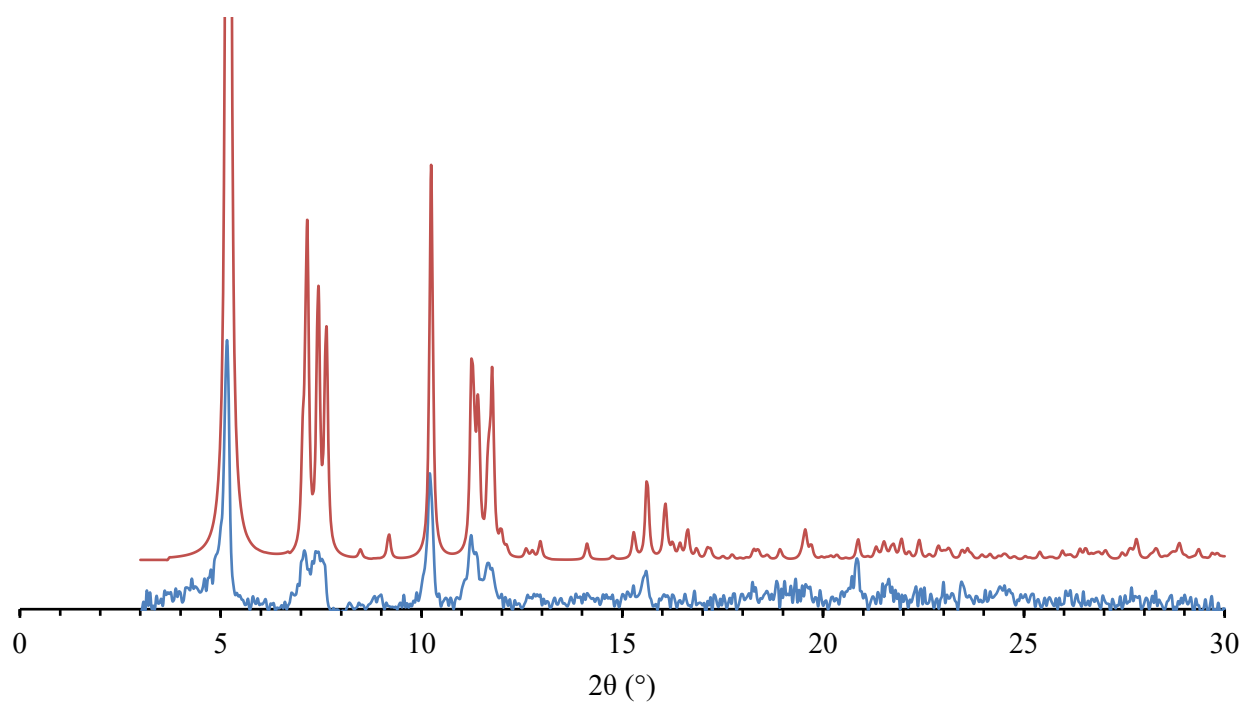


Figure S16: Experimental (blue) and simulated (red) PXRD traces of as-synthesised **WUF-51**. 3-30°, 0.04° step size, 3°/min.

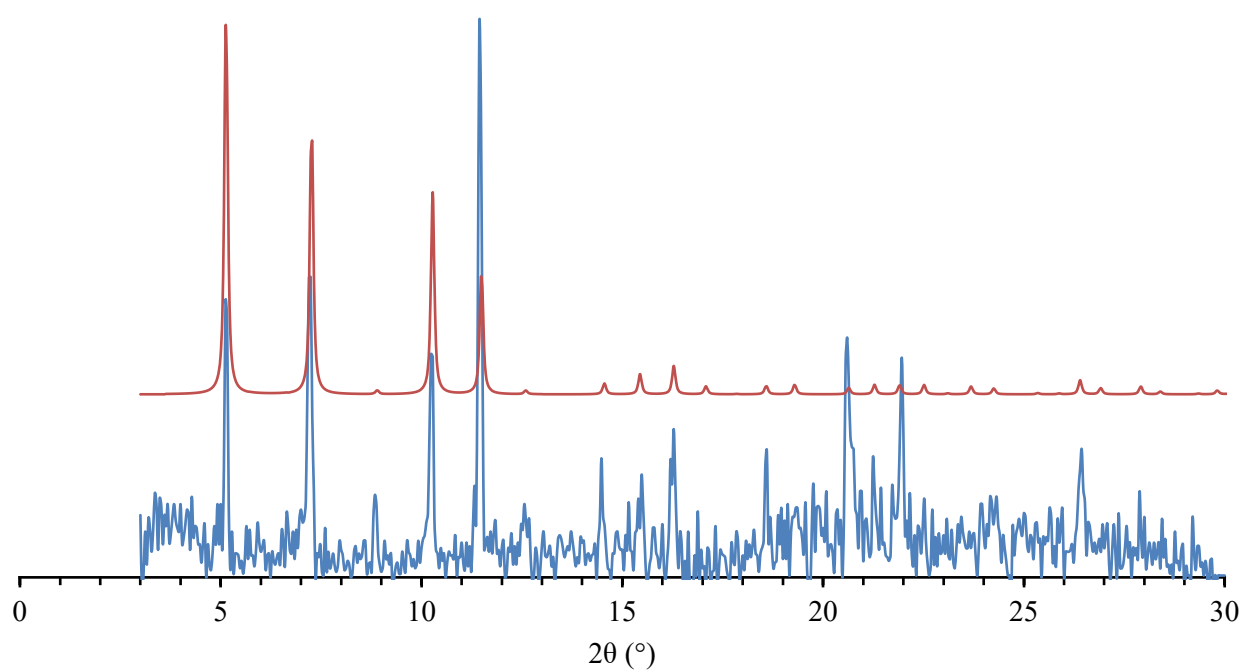


Figure S17: Experimental (blue) and simulated (red) PXRD traces of as-synthesised **WUF-52**. 3-30°, 0.04° step size, 3°/min.

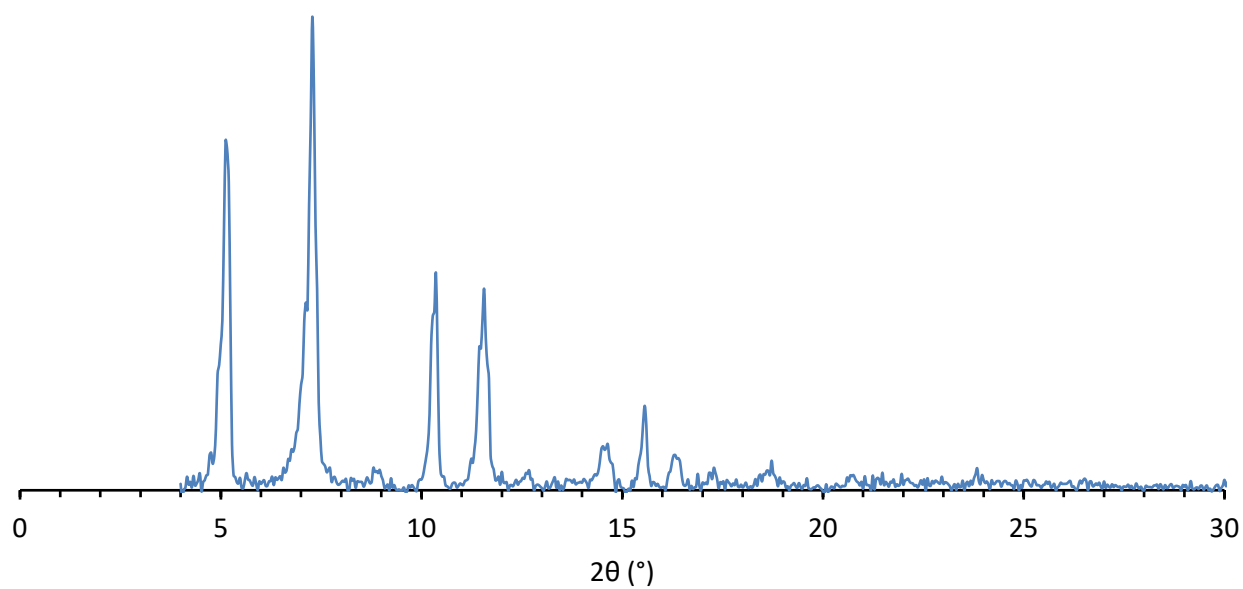
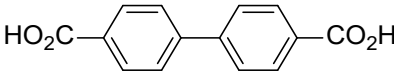
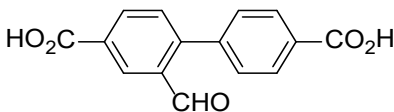
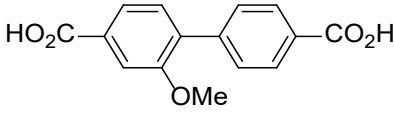
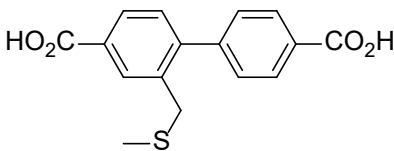
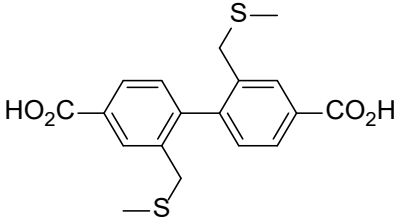
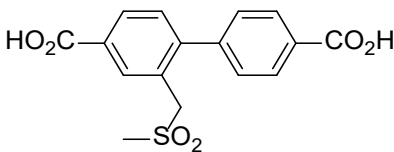
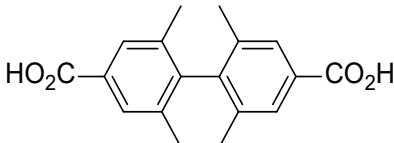
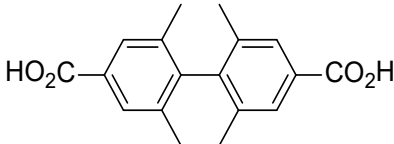
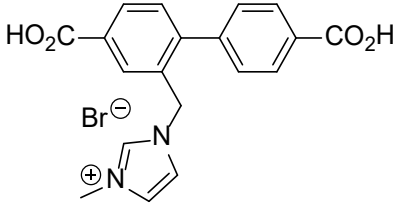


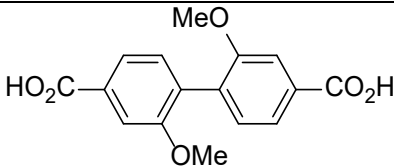
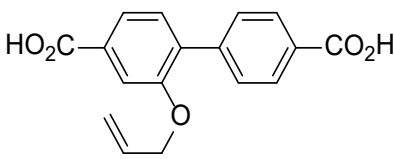
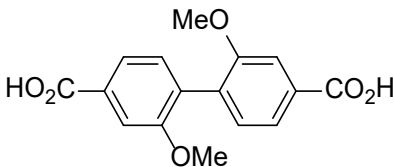
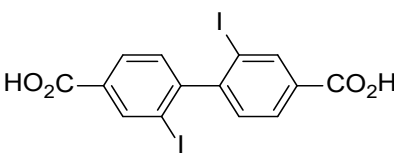
Figure S18: Experimental PXRD trace of as-synthesised **WUF-53**. 3-30°, 0.04° step size, 3°/min.

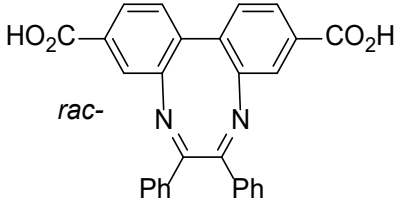
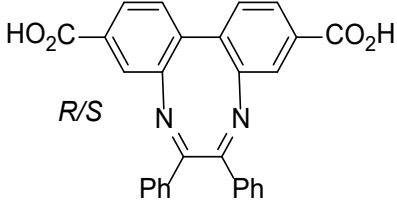
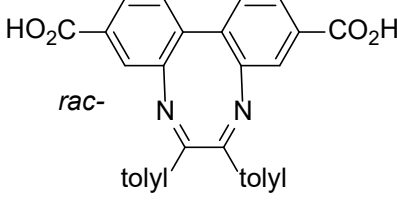
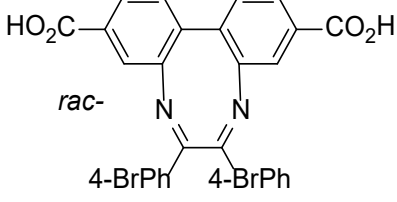
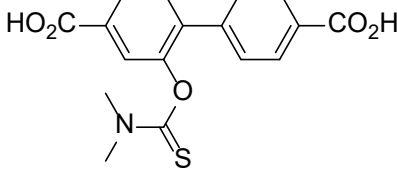
6 Single Crystal X-ray Crystallography

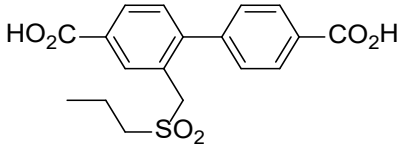
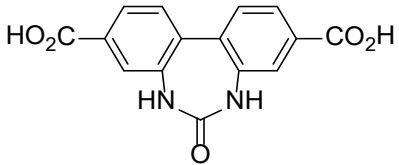
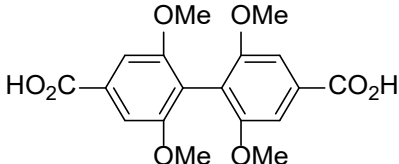
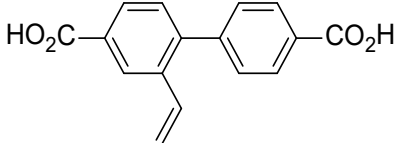
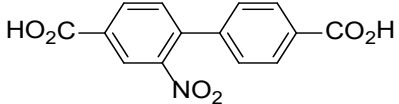
Table S1 Crystallographic data with ligand structures and classifications for IRMOF-9 and functionalised analogues.

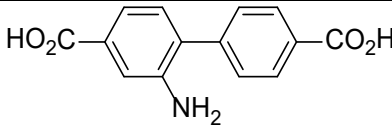
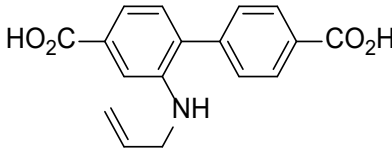
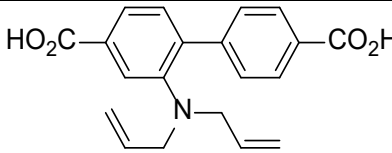
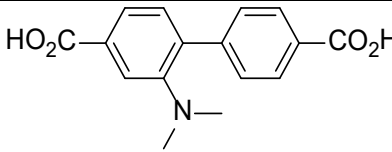
	MOF code	CCDC	Space group	Cell (/Å, °)	Temp. (/K)	Starting Ligand Structure	Type	Reference
1	IRMOF-9	175580	<i>Pnnm</i>	$a = 17.1469(8)$ $b = 23.3222(10)$ $c = 25.2552(12)$ $\alpha = \beta = \gamma = 90$	153(2)		II	M. Eddaoudi, J. Kim, N. Rosi, D. Vodak, J. Wachter, M. O'Keeffe and O. M. Yaghi, <i>Science</i> , 2002, 295 , 469-472.
2		691966	<i>C2/m</i>	$a = 22.7990(19)$ $b = 25.218(3)$ $c = 17.1200(17)$ $\beta = 98.207(4)$	150(2)		III	A. D. Burrows, C. Frost, M. F. Mahon and C. Richardson, <i>Angew. Chem. Int. Ed.</i> , 2008, 47 , 8482-8486.
3	MUF-6	826055	<i>P-42₁m</i>	$a = b = 17.2215(4)$ $c = 17.1168(12)$ $\alpha = \beta = \gamma = 90$	292(2)		II	R. K. Deshpande, G. I. N. Waterhouse, G. B. Jameson and S. G. Telfer, <i>Chem. Commun.</i> , 2012, 48 , 1574-1576.
4		725565	<i>C2/m</i>	$a = 25.0111(9)$ $b = 22.9843(9)$ $c = 17.1959(3)$ $\beta = 96.404(4)$	170(2)		III	A. D. Burrows, C. G. Frost, M. F. Mahon and C. Richardson, <i>Chem. Commun.</i> , 2009, 4218-4220.

5		725566	$R-3m$	$a = b = 23.8212(3)$ $c = 30.2938(11)$ $\alpha = \beta = 90, \gamma = 120$	170(2)		III	A. D. Burrows, C. G. Frost, M. F. Mahon and C. Richardson, <i>Chem. Commun.</i> , 2009, 4218-4220.
6		725567	$C2/m$	$a = 25.1670(4)$ $b = 23.2000(3)$ $c = 17.1020(3)$ $\beta = 93.561(1)$	150(2)		III	A. D. Burrows, C. G. Frost, M. F. Mahon and C. Richardson, <i>Chem. Commun.</i> , 2009, 4218-4220.
7			$R-3c$	$a = b = 22.6523(6)$ $c = 65.9502(16)$ $\alpha = \beta = 90, \gamma = 120$	293(2)		III	T.-H. Park, K. Koh, A. G. Wong-Foy and A. J. Matzger, <i>Cryst. Growth Des.</i> , 2011, 11 , 2059-2063.
8		898759	$R-3c$	$a = b = 22.7345(13)$ $c = 64.308(7)$ $\alpha = \beta = 90, \gamma = 120$	173(2)		III	I. Boldog, L. Xing, A. Schulz and C. Janiak, <i>Comptes Rendus Chimie</i> , 2012, 15 , 866-877.
9			$C2/m$	$a = 24.3627(7)$ $b = 23.9175(7)$ $c = 17.0679(5)$ $\beta = 91.5200(10)$	100(2)		III	J. M. Roberts, O. K. Farha, A. A. Sarjeant, J. T. Hupp and K. A. Scheidt, <i>Cryst. Growth Des.</i> , 2011, 11 , 4747-4750.

10		831357	<i>R</i> -3 <i>m</i>	$a = b = 23.5302(8)$ $c = 31.5110(14)$ $\alpha = \beta = 90, \gamma = 120$	150(2)		III	D. Rankine, A. Avellaneda, M. R. Hill, C. J. Doonan and C. J. Sumby, <i>Chem. Commun.</i> , 2012, 48 , 10328-10330.
11		910203	<i>C</i> 2/ <i>m</i>	$a = 26.0930(15)$ $b = 21.5800(15)$ $c = 17.2380(19)$ $\beta = 92.593(4)$	150(2)		III	A. D. Burrows, S. O. Hunter, M. F. Mahon and C. Richardson, <i>Chem. Commun.</i> , 2013, 49 , 990-992.
12		904635	<i>R</i> -3	$a = b = 23.6899(4)$ $c = 30.8058(7)$ $\alpha = \beta = 90, \gamma = 120$	130(2)		III	W. W. Lestari, P. Lönnecke, M. B. Sárosi, H. C. Streit, M. Adlung, C. Wickleder, M. Handke, W.-D. Einicke, R. Gläser and E. Hey-Hawkins, <i>CrystEngComm</i> , 2013, 15 , 3874.
13		971480	<i>R</i> -3	$a = b = 24.4801(10)$ $c = 29.1304(19)$ $\alpha = \beta = 90, \gamma = 120$	150(2)		III	R. Babarao, C. J. Coghlan, D. Rankine, W. M. Bloch, G. K. Gransbury, H. Sato, S. Kitagawa, C. J. Sumby, M. R. Hill and C. J. Doonan, <i>Chem. Commun.</i> , 2014, 50 , 3238-3241.

14	β -MUF-9	1437610	$Pn-3m$	$a = b = c = 17.0842(9)$ $\alpha = \beta = \gamma = 90$	153(2)		I	A. Ferguson, L. Liu, S. J. Tapperwijn, D. Perl, F. X. Coudert, S. Van Cleuvenbergen, T. Verbiest, M. A. van der Veen and S. G. Telfer, <i>Nat. Chem.</i> , 2016, 8 , 250-257.
15	(R/S)- β -MUF-10	1437611	$P4_232$	$a = b = c = 17.188(4)$ $\alpha = \beta = \gamma = 90$	293(2)		I	A. Ferguson, L. Liu, S. J. Tapperwijn, D. Perl, F. X. Coudert, S. Van Cleuvenbergen, T. Verbiest, M. A. van der Veen and S. G. Telfer, <i>Nat. Chem.</i> , 2016, 8 , 250-257.
16	β -MUF-11	1438094	$Pn-3m$	$a = b = c = 17.0462(9)$ $\alpha = \beta = \gamma = 90$	143(2)		I	A. Ferguson, L. Liu, S. J. Tapperwijn, D. Perl, F. X. Coudert, S. Van Cleuvenbergen, T. Verbiest, M. A. van der Veen and S. G. Telfer, <i>Nat. Chem.</i> , 2016, 8 , 250-257.
17	β -MUF-12	1438095	$Pn-3m$	$a = b = c = 17.1820(6)$ $\alpha = \beta = \gamma = 90$	293(2)		I	A. Ferguson, L. Liu, S. J. Tapperwijn, D. Perl, F. X. Coudert, S. Van Cleuvenbergen, T. Verbiest, M. A. van der Veen and S. G. Telfer, <i>Nat. Chem.</i> , 2016, 8 , 250-257.
18	WUF-1	1501497	$C2/m$	$a = 24.670(5)$ $b = 23.940(4)$ $c = 17.201(5)$	292		III	T. A. Ablott, M. Turzer, S. G. Telfer and C. Richardson, <i>Cryst. Growth Des.</i> , 2016, 16 , 7067-7073.

				$\beta = 91.221(15)$				
19	WUF-10	1503491	$C2/m$	$a = 24.6493(15)$ $b = 24.0029(12)$ $c = 17.2267(12)$ $\beta = 91.311(6)$	292		III	M. R. Bryant, A. D. Burrows, C. J. Kepert, P. D. Southon, O. T. Qazvini, S. G. Telfer and C. Richardson, <i>Cryst. Growth Des.</i> , 2017, 17 , 2016-2023.
20		1563596	$R-3c$	$a = b = 24.4635(15)$ $c = 112.996(8)$ $\alpha = \beta = 90, \gamma = 120$			III	S. Glomb, D. Woschko, G. Makhloufi and C. Janiak, <i>ACS App. Mater. Interfaces</i> , 2017, 9 , 37419-37434.
21		1448509	$R-3$	$a = b = 24.763(5)$ $c = 28.146(9)$ $\alpha = \beta = 90, \gamma = 120$	100(2)			J. Li, Y. Ren, C. Qi and H. Jiang, <i>Eur. J. Inorg. Chem.</i> , 2017, 11 , 1478-1487.
22	WUF-19	1872644	$C2/m$	$a = 24.468$ $b = 24.0292$ $c = 17.1491$ $\beta = 90.869$	292(1)		III	M. R. Bryant, T. A. Ablott, S. G. Telfer, L. Liu and C. Richardson <i>CrystEngComm</i> , 2019, 21 , 60–64.
23	WUF-22(14)	1912370	$C2/m$	$a = 24.3610(12)$ $b = 24.2585(10)$ $c = 17.2141(12)$	292(1)		III	L. Conte, T.-Y. Zhou, O. T. Qazvini, L. Liu, D. R. Turner, S. G. Telfer and C. Richardson, <i>Aust. J. Chem.</i> , 2019, 72 , 811-816.

				$\beta = 91.458(6)$				
24	WUF-11	1944583	$P-42_1m$	$a = b = 17.2045(5)$ $c = 17.1507(12)$ $\alpha = \beta = \gamma = 90$	293(2)		II	A. Khansari, M. R. Bryant, D. R. Jenkinson, G. B. Jameson, O. T. Qazvini, L. Liu, A. D. Burrows, S. G. Telfer and C. Richardson, <i>CrystEngComm</i> , 2019, 21 , 7498.
25	WUF-12	1944584	$P-42_1m$	$a = b = 17.237(2)$ $c = 17.1207(17)$ $\alpha = \beta = \gamma = 90$	293(2)		II	A. Khansari, M. R. Bryant, D. R. Jenkinson, G. B. Jameson, O. T. Qazvini, L. Liu, A. D. Burrows, S. G. Telfer and C. Richardson, <i>CrystEngComm</i> , 2019, 21 , 7498.
26	WUF-13	1944585	$P-42_1m$	$a = b = 17.2000(12)$ $c = 17.2000(12)$ $\alpha = \beta = \gamma = 90$	293(2)		II	A. Khansari, M. R. Bryant, D. R. Jenkinson, G. B. Jameson, O. T. Qazvini, L. Liu, A. D. Burrows, S. G. Telfer and C. Richardson, <i>CrystEngComm</i> , 2019, 21 , 7498.
27	WUF-14	1944586	$R-3m$	$a = b = 24.106(3)$ $c = 30.383(3)$ $\alpha = \beta = 90, \gamma = 120$	293(2)		III	A. Khansari, M. R. Bryant, D. R. Jenkinson, G. B. Jameson, O. T. Qazvini, L. Liu, A. D. Burrows, S. G. Telfer and C. Richardson, <i>CrystEngComm</i> , 2019, 21 , 7498.

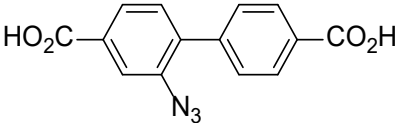
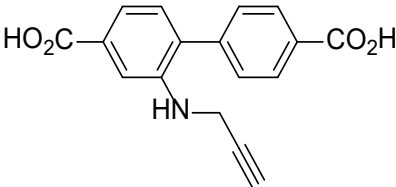
28	WUF-51	Not deposited. Data available from the authors.	$C2/m$	$a = 25.102(4)$ $b = 223.165(3)$ $c = 17.288(2)$ $\beta = 93.191(8)$	292(1)		III	This work
29	WUF-52	2022084	$P-42_1m$	$a = b = 17.2000(12)$ $c = 17.2000(12)$ $\alpha = \beta = \gamma = 90$	292(1)		II	This work

Table S2. Crystal data and structure refinement for 1,4 Me₄L^{Triaz}.

Identification code	1,4 Me ₄ L ^{Triaz} (exp_197_MF2)
Empirical formula	C ₃₅ H ₃₀ N ₄ O ₈
Formula weight	634.63
Temperature/K	293(1)
Crystal system	triclinic
Space group	P-1
a/Å	10.5406(3)
b/Å	10.8847(2)
c/Å	13.6301(4)
α/°	94.515(2)
β/°	101.132(2)
γ/°	96.424(2)
Volume/Å ³	1516.65(7)
Z	2
ρ _{calc} /g/cm ³	1.390
μ/mm ⁻¹	0.100
F(000)	664.0
Crystal size/mm ³	0.326 × 0.237 × 0.201
Radiation	MoKα (λ = 0.71073)
2θ range for data collection/°	4.494 to 58.26
Index ranges	-14 ≤ h ≤ 14, -14 ≤ k ≤ 14, -18 ≤ l ≤ 18
Reflections collected	79549
Independent reflections	8018 [R _{int} = 0.0346, R _{sigma} = 0.0209]
Data/restraints/parameters	8018/0/432
Goodness-of-fit on F ²	1.057
Final R indexes [I ≥ 2σ (I)]	R ₁ = 0.0429, wR ₂ = 0.1136
Final R indexes [all data]	R ₁ = 0.0628, wR ₂ = 0.1249
Largest diff. peak/hole / e Å ⁻³	0.23/-0.17
CCDC	2022085

Notes:

This molecule crystallizes in the space group *P*-1 with a single 1,4-regioisomer in the asymmetric unit. All bond lengths are within expected ranges. The hydrogen attached to the amine was refined. All other hydrogens were positioned geometrically and allowed to ride on their carrier carbons.

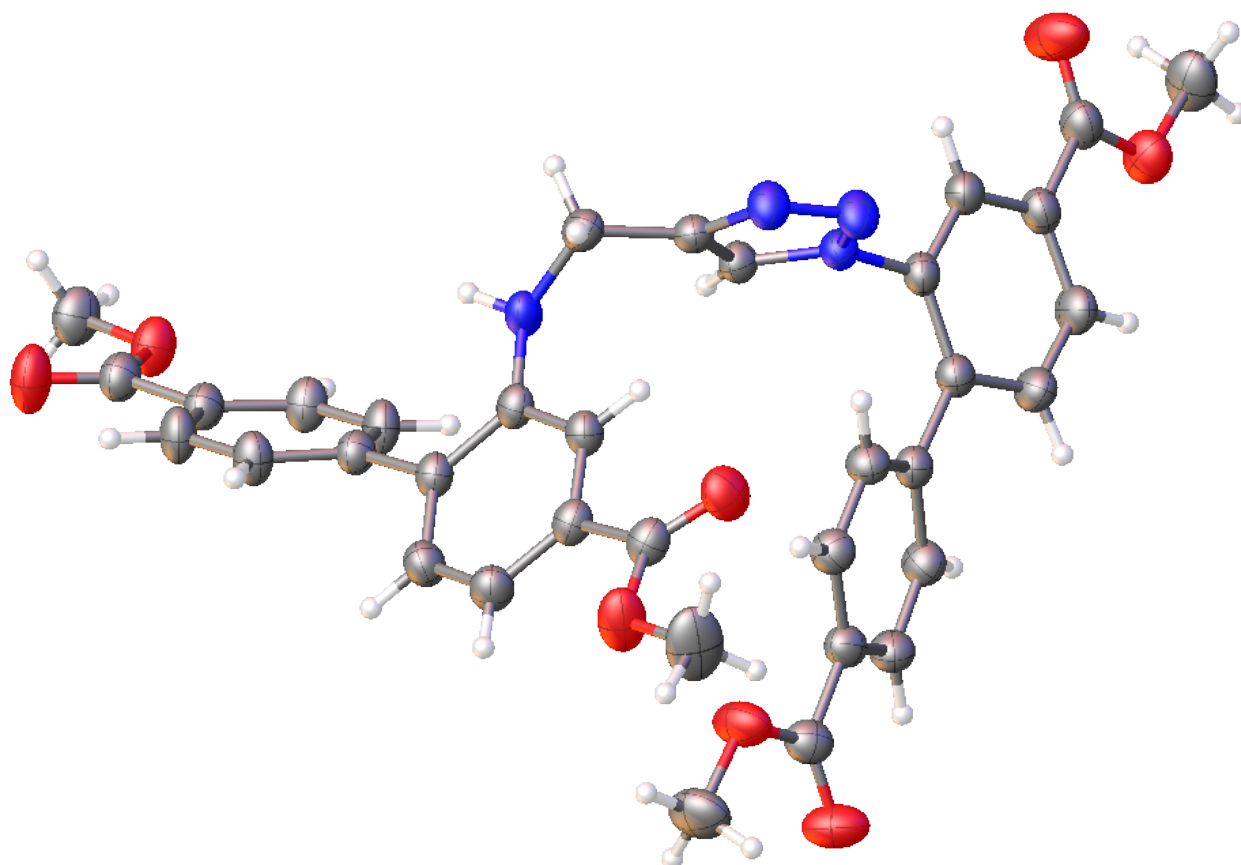


Figure S19: Crystal structure of $\text{Me}_4\text{L}^{\text{Traiz}}$ with displacement ellipsoids at 50%. Carbon atoms are grey; oxygen atoms are red; nitrogen atoms are blue; hydrogen atoms are white.

Table S3. Crystal data and structure refinement for **WUF-52** ($\text{Zn}_4\text{O}(\text{bpdCNHCH}_2\text{C}\equiv\text{CH})_3$)

Identification code	WUF-52
Empirical formula	$\text{C}_{51}\text{H}_{33}\text{N}_3\text{O}_{13}\text{Zn}_4$
Formula weight	1157.28
Temperature/K	292
Crystal system	tetragonal
Space group	$P-42_1m$
$a/\text{\AA}$	17.2000(12)
$b/\text{\AA}$	17.2000(12)
$c/\text{\AA}$	17.2000(12)
$\alpha/^\circ$	90
$\beta/^\circ$	90
$\gamma/^\circ$	90
Volume/ \AA^3	5088.4(8)
Z	2
$\rho_{\text{calc}}/\text{g cm}^{-3}$	0.755
μ/mm^{-1}	1.346
$F(000)$	1168.0
Crystal size/ mm^3	$0.1 \times 0.1 \times 0.1$
Radiation	$\text{CuK}\alpha$ ($\lambda = 1.54178$)
2θ range for data collection/ $^\circ$	11.504 to 117.8
Index ranges	$-15 \leq h \leq 14, -16 \leq k \leq 19, -19 \leq l \leq 19$
Reflections collected	28491
Independent reflections	3824 [$R_{\text{int}} = 0.2457, R_{\text{sigma}} = 0.1933$]
Data/restraints/parameters	3824/149/154
Goodness-of-fit on F^2	1.088
Final R indexes [$I \geq 2\sigma(I)$]	$R_1 = 0.1015, wR_2 = 0.2332$
Final R indexes [all data]	$R_1 = 0.1106, wR_2 = 0.2487$
Largest diff. peak/hole / $e \text{\AA}^{-3}$	0.57/-0.65
Flack parameter	0.37(4)
CCDC	2022084

Notes:

This framework crystallizes in the space group $P-42_1m$ and was refined as a three-component twin (0 0 1, 1 0 0, 0 1 0; 1, 0.426(9); 2, 0.271(6); 3, 0.303(6)). The crystal system is tetragonal but metrically cubic – crystals extinguish under cross polarised light therefore they cannot be crystallographically cubic. The Flack test then represents a mixture of enantiomeric forms in the trilled crystals. We discuss related twinning problems in a previous article.⁹ The data were collected using rotating anode generated $\text{Cu K}\alpha$ radiation at room temperature with the crystal in a solvent-filled polymer sheath. In our experience the diffraction was quite good for this sample and the data were truncated in the refinement to a resolution of 0.9. The R_{int} statistic is quite high at 0.24 and is affected by the trilling

⁹A. Khansari, M. R. Bryant, D. R. Jenkinson, G. B. Jameson, O. T. Qazvini, L. Liu, A. D. Burrows, S. G. Telfer and C. Richardson, *CrystEngComm*, 2019, **21**, 7498-7506.

of the sample. Nevertheless, the refinement is okay and the structure is sensible and consistent with many of our other single crystal structures of similar MOFs.

The asymmetric unit (ASU) of this structure is shown in Fig. S20 and contains two zinc ions of half site occupancy bound to two unique carboxylate groups and an oxido anion of quarter site occupancy. The SBU straddles two mirror planes and this generates the tetrazinc node with an overall octahedral geometry coordinated by six carboxylate groups from bridging ligands.

Oxygen atoms O2, O3 and carbons C1-C7 are full site occupancy within the ASU and straddle two perpendicular glide planes parallel to the *c*-axis that generate the remainder of the ligand. Oxygen atoms O4, O5 and carbons C7-C13 are half-site occupancy and straddle two perpendicular mirror planes, also parallel to the *c*-axis, that generate the remainder of the ligand.

Pendent propargylamine groups on the biphenyl linkers (-NH-CH₂-C≡CH) could not be fully located on Fourier difference maps and their positions and thermal parameters were fixed with sensible bond distances (e.g. C≡C, 1.20 Å). The occupancies were also fixed to match the site symmetry of the positions. The pendent groups were not included in the structural refinement. Bonds connecting these groups to their aromatic rings were subject to a DFIX restraint (1.4(0.01) Å).

Phenyl ring C8(C9,C10,C11,C12,C13) fitted as a hexagon and refined as free rotating group. The phenyl ring based on C25-C28 was restrained to be approximately planar and with a similarity restraint to the regular phenyl ring based on C8-C13. Most carbons and all oxygens are under a SIMU restraint Uiso/Uaniso. Hydrogen atoms were placed geometrically and in riding models.

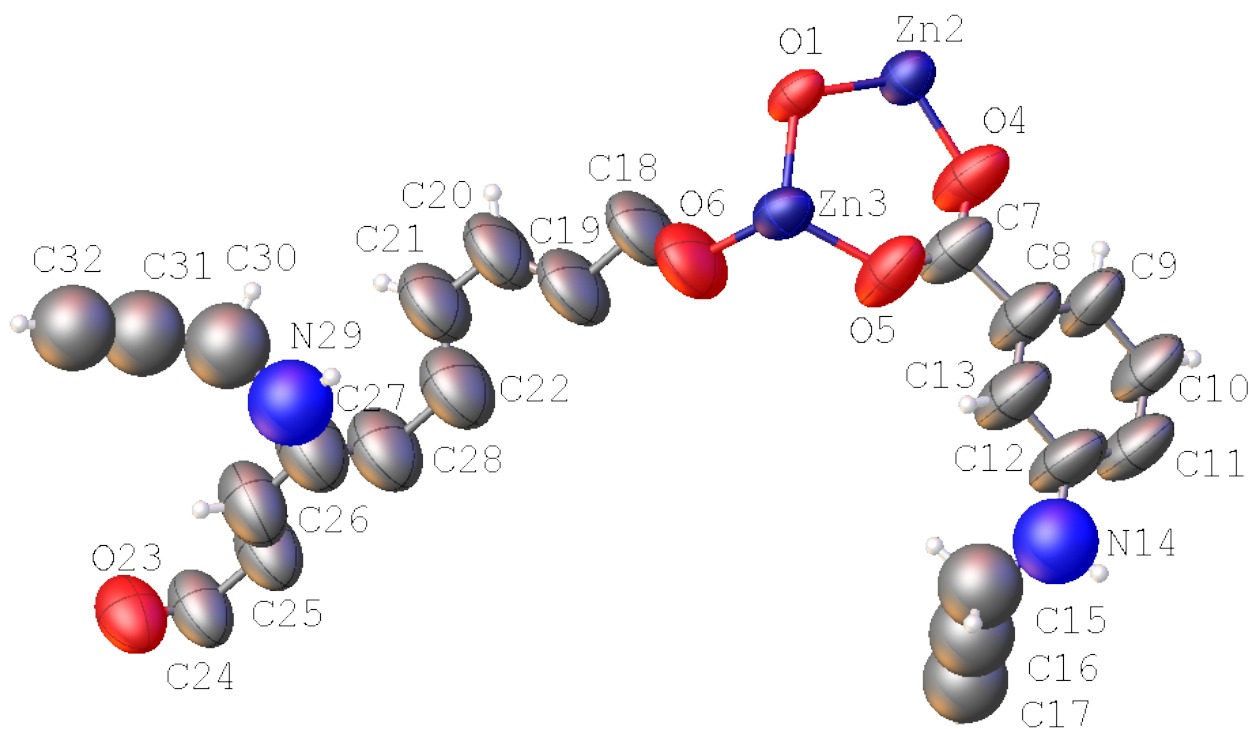


Figure S20 Image of the asymmetric unit of **WUF-52** with displacement ellipsoids at the 50% probability level for anisotropically refined atoms and with fixed Uiso of 0.2 for the pendent tag groups.

Table S4. Crystal data and structure refinement for as synthesized **WUF-51** $\text{Zn}_4\text{O}(\text{bpdcN}_3)_3(\text{DMF})_2$.

Identification code	CRazide_0m
Empirical formula	$\text{C}_{48}\text{H}_{35}\text{N}_{11}\text{O}_{15}\text{Zn}_4$
Formula weight	1267.35
Temperature/K	293.15
Crystal system	Monoclinic
Space group	$C2/m$
a/Å	25.102(4)
b/Å	23.165(3)
c/Å	17.288(2)
$\alpha/^\circ$	90
$\beta/^\circ$	93.191(8)
$\gamma/^\circ$	90
Volume/Å ³	10037(2)
Z	4
$\rho_{\text{calc}}/\text{g cm}^{-3}$	0.839
μ/mm^{-1}	1.433
F(000)	2560.0
Crystal size/mm ³	? × ? × ?
Radiation	$\text{CuK}\alpha$ ($\lambda = 1.54178$)
2 θ range for data collection/ $^\circ$	11.258 to 79.932
Index ranges	$-20 \leq h \leq 20, -18 \leq k \leq 19, -14 \leq l \leq 14$
Reflections collected	20772
Independent reflections	3156 [$R_{\text{int}} = 0.1908, R_{\text{sigma}} = 0.1341$]
Data/restraints/parameters	3156/539/265
Goodness-of-fit on F^2	1.090
Final R indexes [$I \geq 2\sigma(I)$]	$R_1 = 0.1043, wR_2 = 0.2824$
Final R indexes [all data]	$R_1 = 0.1327, wR_2 = 0.3010$
Largest diff. peak/hole / e Å ⁻³	1.28/-0.71

Notes:

The data were collected using a Cu K α radiation at room temperature with the crystal in a solvent-filled polymer sheath. The data are weak (resolution cut at 1.2 Å) and there is quite a lot of disorder in the structure. The Rint statistic is quite high at 0.19 and this is not a quality dataset. No crystal size was measured at the time of diffraction and the data is available from the authors (chris_richardson@uow.edu.au). The structural analysis gives a sensible structure in a common space group for this type of MOF (see Table S1).

This framework crystallizes in the space group $C2/m$. The asymmetric unit of this structure contains one full occupancy zinc ion, two zinc ions of half site occupancy, an oxido atom of half site occupancy, one and a half bpdc-N₃ ligands, and two DMF ligands coordinated to Zn²⁺. The Zn₄O SBU is generated by a mirror plane that passes between Zn1 and Zn2. The DMF ligands are disordered across the mirror plane as is one of the phenyl rings bearing an azide tag group (see Figure S21)

The structure required extensive modelling and restraints/constraints. All anisotropically-refined atoms were placed under a RIGU command and an ISOR command was used for all oxygen and carbons atoms. Phenyl rings C8-C13 and C17-C22 were modeled as rotatable hexagons. The phenyl ring C29-C34 was regularized with SADI and FLAT restraints and some displacement ellipsoids were constrained to be the same with EADP commands. The SAME command using C7-C11 was used to help the geometries of C36-C40. Aromatic hydrogen atoms were placed geometrically.

The DMF ligands were imported as rigid groups and then the atoms were fixed in position and displacement parameters. A FLAT command was used for C6D O2 N7D C9D C8D. The methyl hydrogen atoms on the DMF ligands were fixed (AFIX 31).

Parts of the azide groups were found in the difference maps and were completed by adding atoms in the ASU with sensible bond lengths. After further modelling, the atom sites, site occupancy factors and displacement parameters were fixed.

7 TG–DSC data

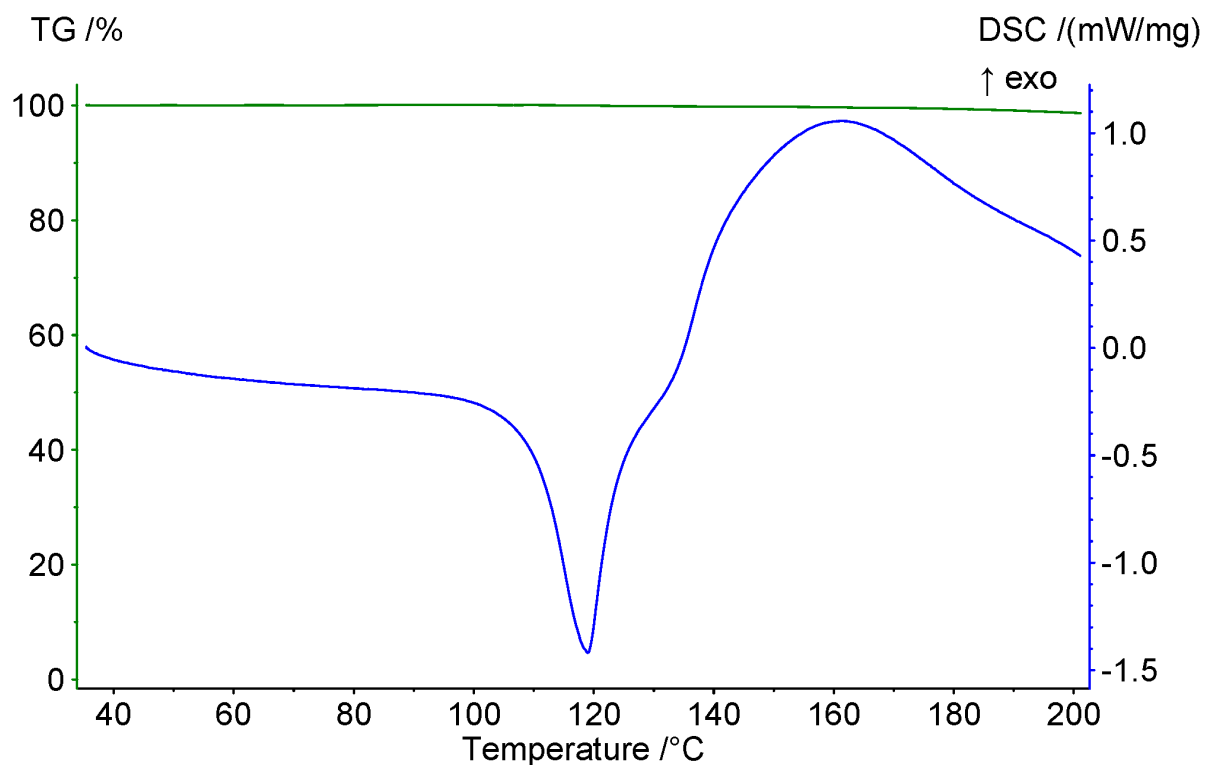


Figure S22: DSC-TGA trace for heating an equimolar mixture of $\text{Me}_2\text{bpdCN}_3$ and $\text{Me}_2\text{bpdCNHCH}_2\text{C}\equiv\text{CH}$ under N_2 gas flow to 200 °C. The TGA trace is shown in green and the DSC trace in blue. The endotherm begins at 110 °C and is indicative of the esters melting. The exotherm onset occurs at 134 °C with no mass loss and is evidence for triazole formation.

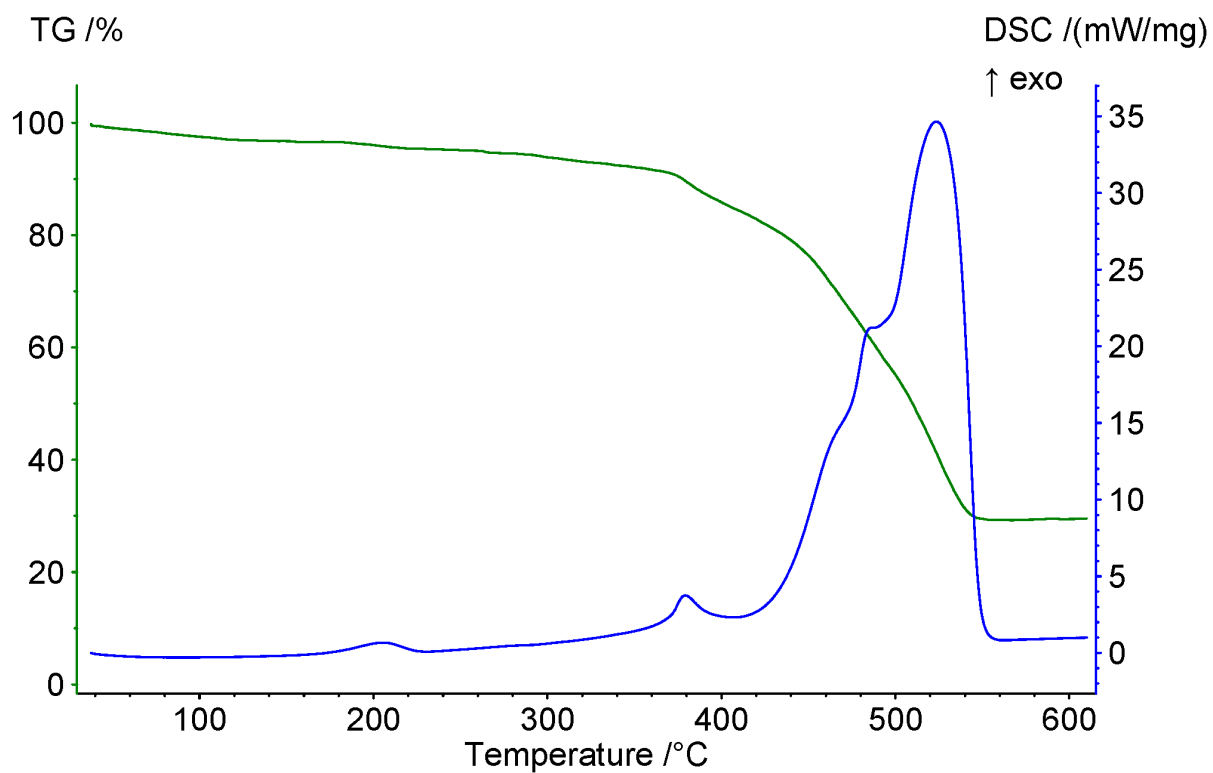


Figure S23: DSC-TGA trace for heating **WUF-50** under flow of 20% O₂ in N₂. The TGA trace is shown in green and the DSC trace in blue. The onset for the Huisgen cycloaddition occurs at 170 °C. Residual mass corresponds to ZnO (calc. 28.6%; found 29.7%).

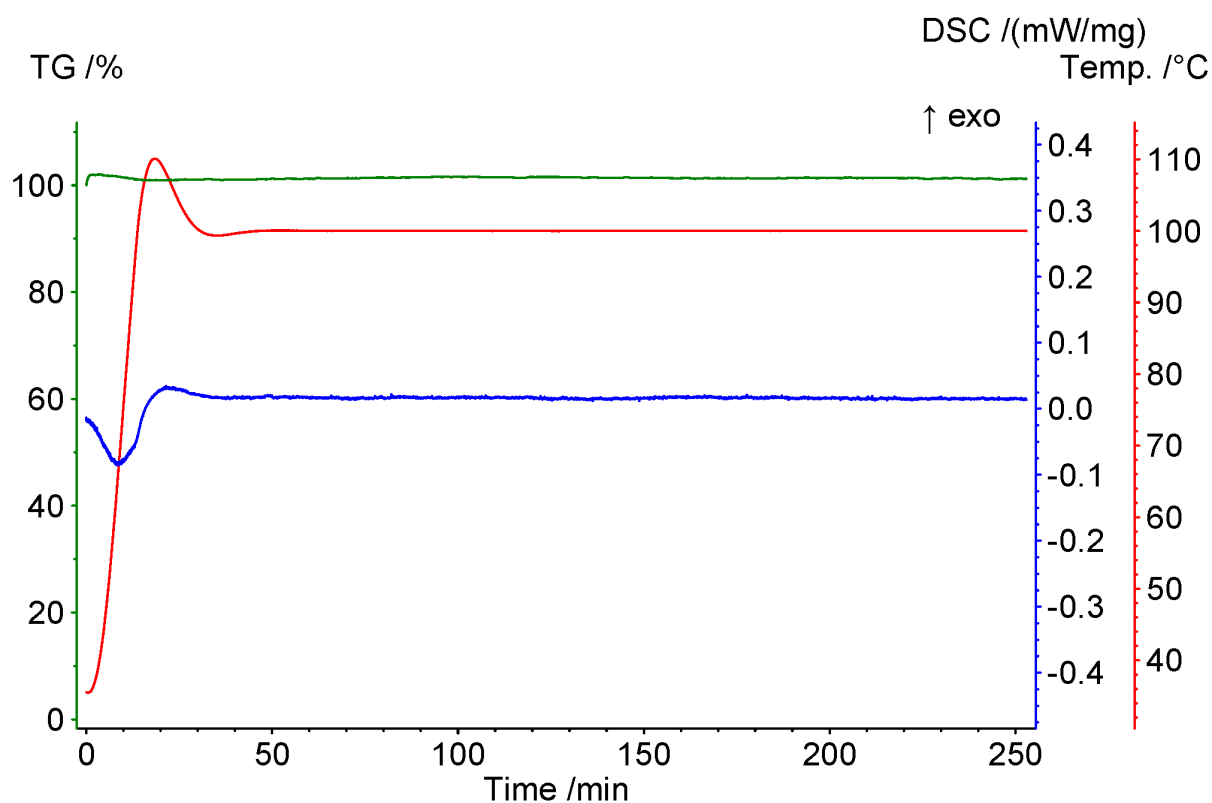


Figure S24: DSC-TGA for heating **WUF-50** to 90 °C under a N₂ atmosphere for four hours. The TGA trace is shown in green, the DSC trace in blue, and the temperature in red. No mass loss is observed. This is evidence for no thermal linking during activation or degassing for gas adsorption analysis.

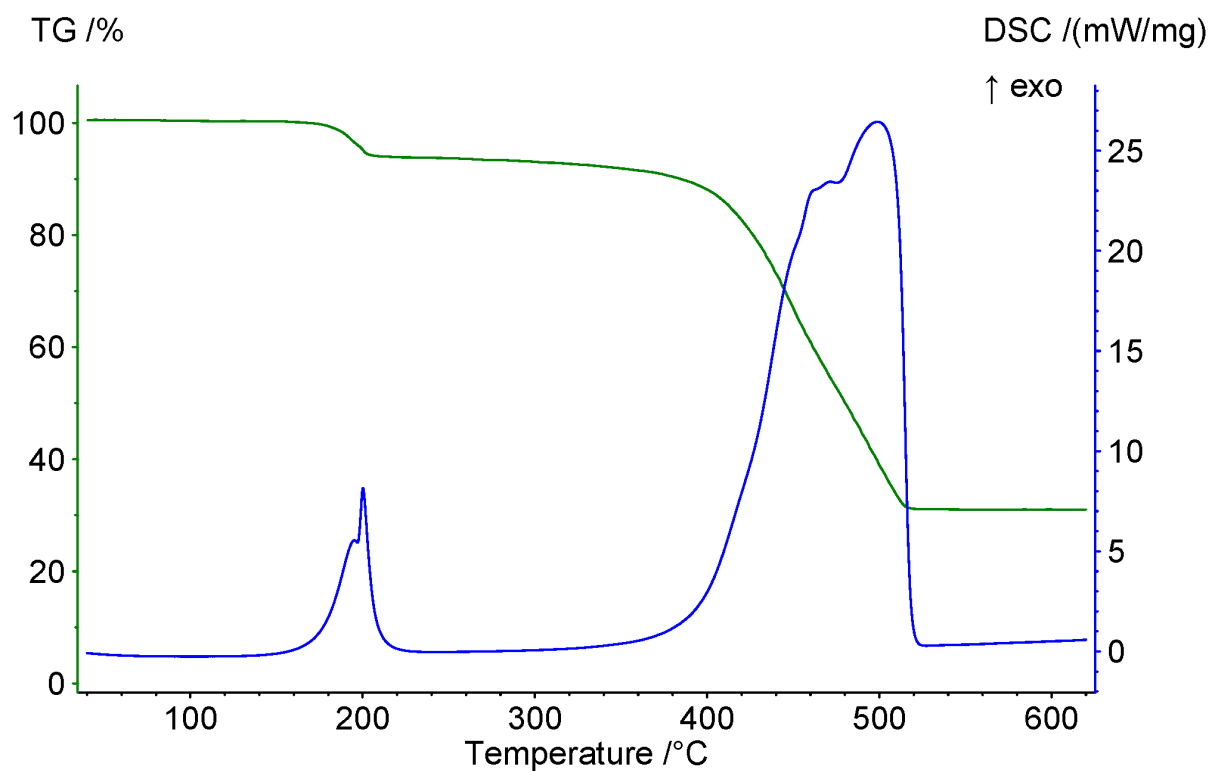


Figure S25: DSC-TGA trace for heating **WUF-51** under flow of 20% O₂ in N₂. The TG trace is shown in green and the DSC trace in blue. Mass loss at 176 °C corresponds to elimination of N₂ from the azide groups (calc. 7.5%; found 6.9%). Residual mass corresponds with ZnO (calc. 29.0%; found 31.0%).

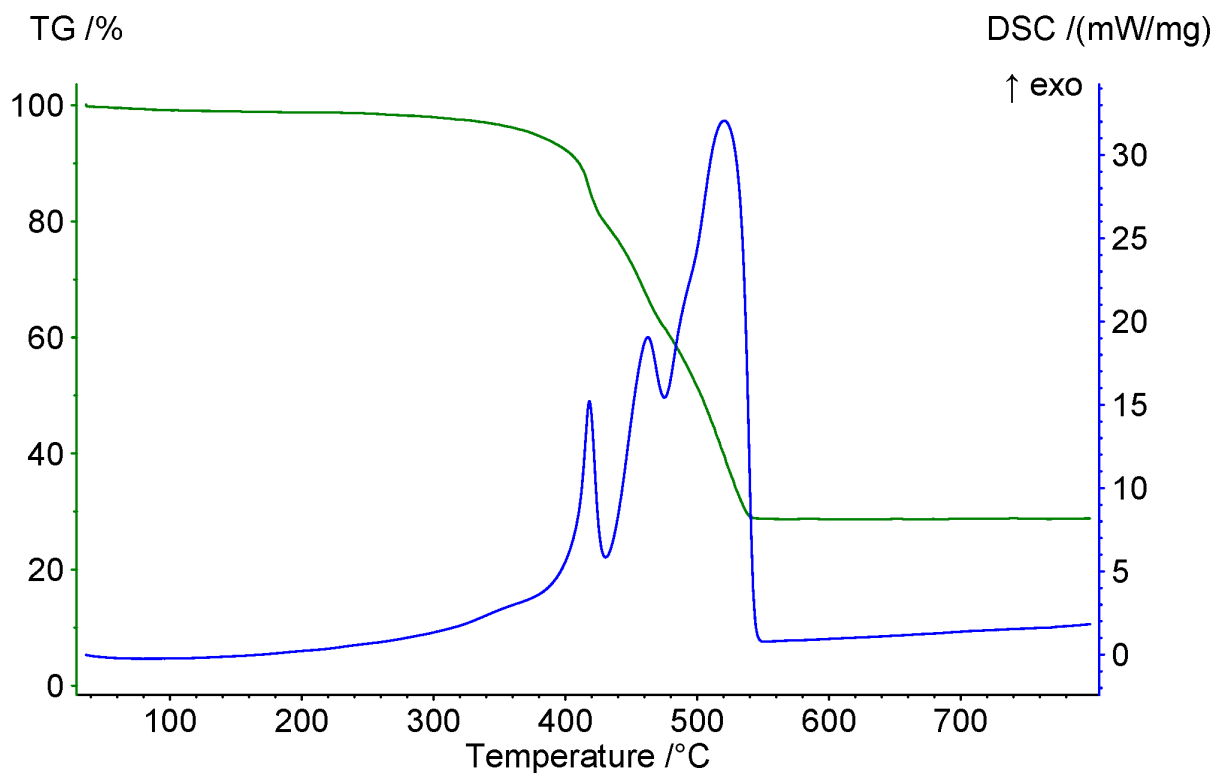


Figure S26: DSC-TGA trace for heating **WUF-52** under a flow of 20% O₂ in N₂. The TGA trace is shown in green and the DSC trace in blue. The framework first experiences mass loss at 300 °C before decomposing in three exothermic events above 350 °C. Residual mass corresponds with ZnO (calc. 28.1%; found 28.8%).

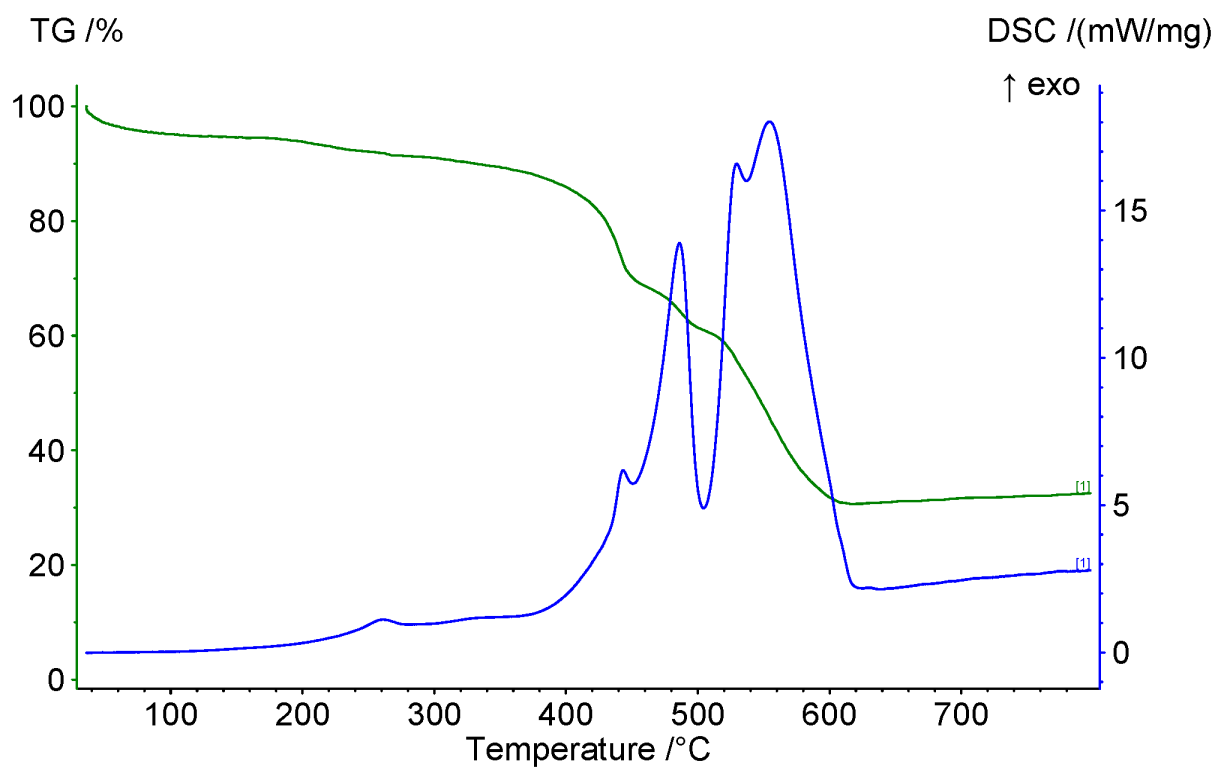


Figure S27: DSC-TGA trace for heating **WUF-53** under a flow of 20% O₂ in N₂. The TGA trace is shown in green and the DSC trace in blue. The framework decomposes in four exothermic events above 425 °C. Residual mass corresponds with ZnO (calc. 28.6%; found 32.5%).

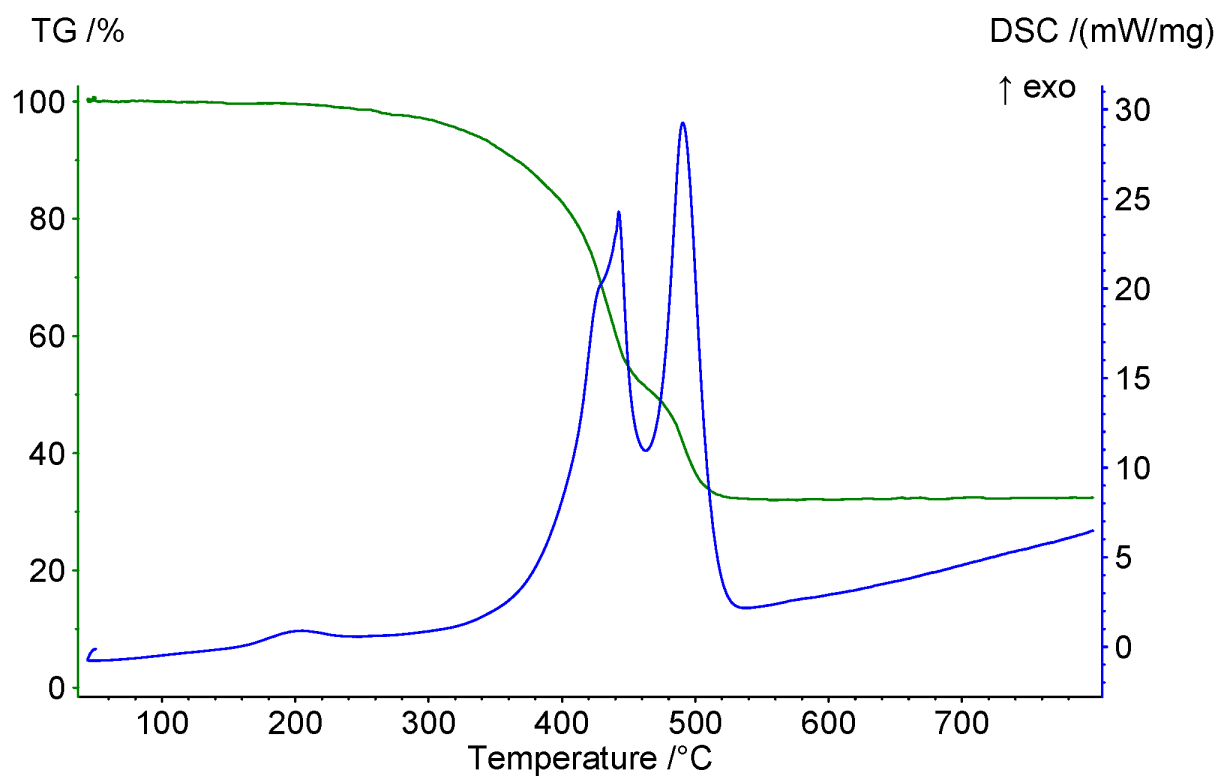


Figure S28: DSC-TGA trace for heating PS-WUF-54 under a flow of 20% O₂ in N₂. The TG trace is shown in green and the DSC trace in blue. The small exotherm starting at ~170 °C most likely reflects the ~4% remaining azide functionality from heating the framework to 200 °C to generate this MOF. The framework starts to undergo decomposition from 300 °C before major decomposition in two exothermic events above 400 °C. Residual mass corresponds with ZnO (calc. 31.4%; found 32.4%).

8 Gas Adsorption Isotherms and Surface Area Calculations

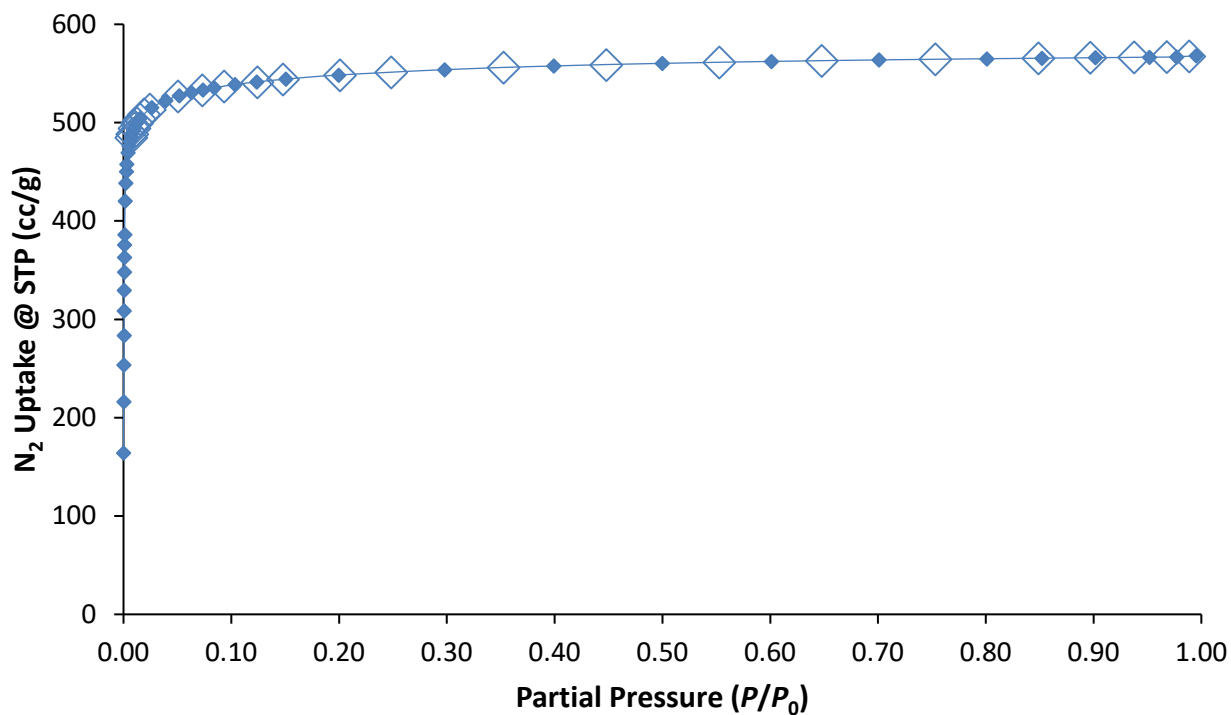


Figure S29: N₂ gas adsorption isotherm at 77 K for **WUF-50**. Adsorption shown in solid diamonds; desorption hollow diamonds.

BET summary		WUF-50 19-058
Slope =		1.578
Intercept =		5.326E-04
Correlation coefficient, r =		0.999995
C constant =		2963.432
Surface Area =		2206.522 m ² /g
Relative Pressure P/Po	Volume @ STP (cc/g)	1 / [W((Po/P) - 1)]
8.08992E-03	489.4184	1.3333E-02
9.07531E-03	492.3300	1.4884E-02
1.00697E-02	494.8311	1.6448E-02
1.20915E-02	499.8795	1.9591E-02
1.50478E-02	504.4843	2.4230E-02
2.60085E-02	515.2719	4.1464E-02
3.91146E-02	522.6683	6.2315E-02

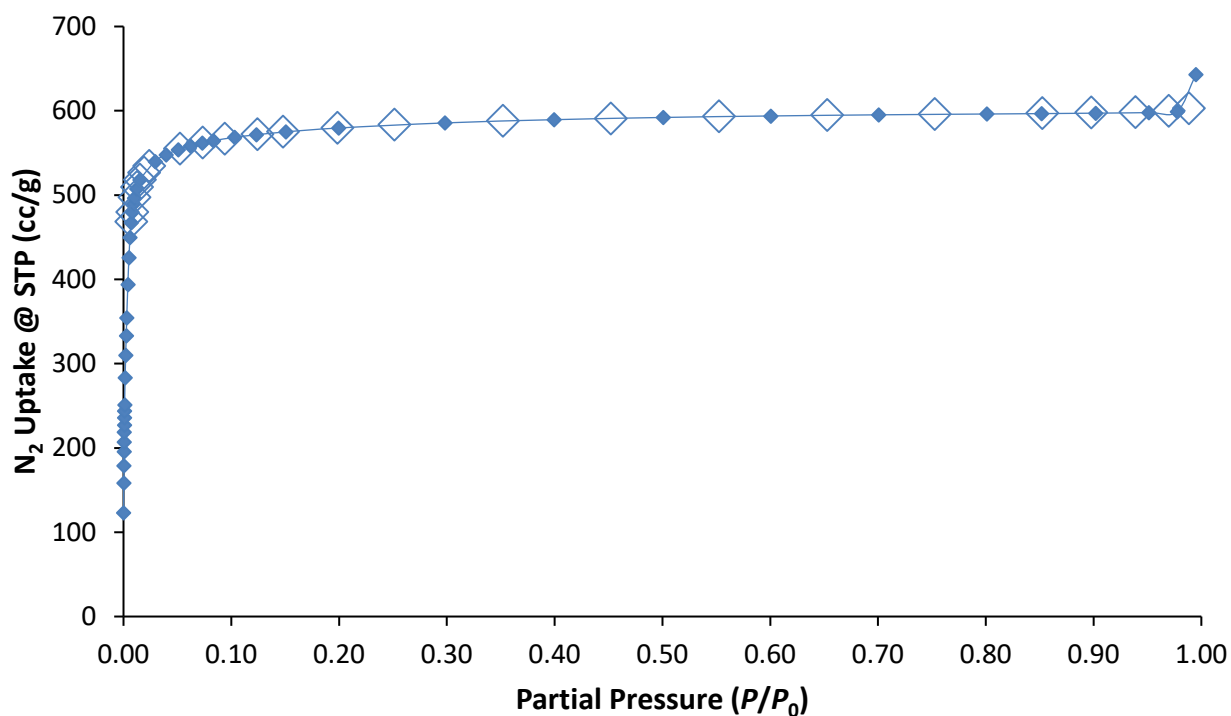


Figure S30: N₂ gas adsorption isotherm at 77 K for **WUF-51**. Adsorption shown in solid diamonds; desorption hollow diamonds. Surface area 2350 m²g⁻¹.

BET summary		WUF-51 19-061
Slope =		1.48
Intercept =		1.466E-03
Correlation coefficient, r =		0.999981
C constant =		1010.53
Surface Area =		2350.372 m ² /g
Relative Pressure P/Po	Volume @ STP (cc/g)	1 / [W((Po/P) - 1)]
7.99726E-03	479.8284	1.3443E-02
9.06169E-03	489.7758	1.4939E-02
9.98971E-03	496.3958	1.6264E-02
1.20358E-02	507.5129	1.9206E-02
1.51439E-02	518.094	2.3747E-02
2.92335E-02	539.8908	4.4628E-02
3.93940E-02	547.8702	5.9890E-02

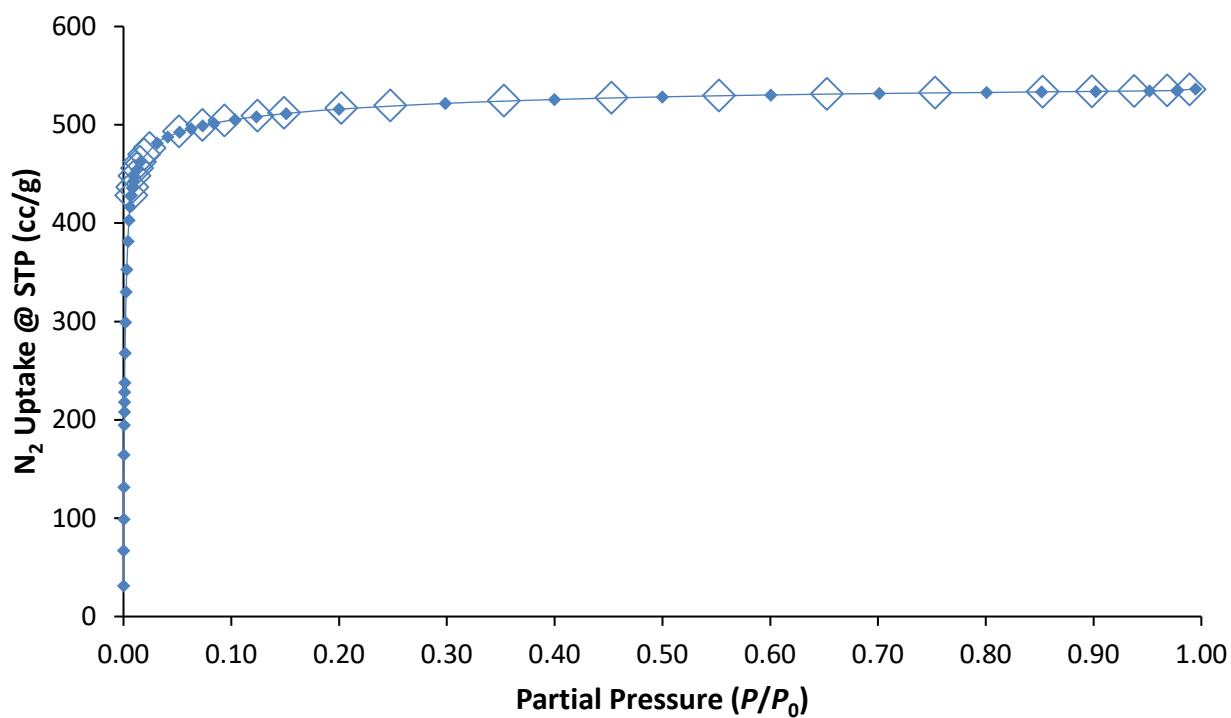


Figure S31: N₂ gas adsorption isotherm at 77 K for **WUF-52**. Adsorption shown in solid diamonds, desorption hollow diamonds. Surface area 2076 m²g⁻¹.

BET summary		WUF-52 17-069
Slope =		1.676
Intercept =		1.31E-03
Correlation coefficient, r =		0.999993
C constant =		1282.02
Surface Area =		2075.782 m ² /g
Relative Pressure P/Po	Volume @ STP (cc/g)	1 / [W((Po/P) - 1)]
8.00858E-03	435.907	1.4819E-02
9.11813E-03	442.8545	1.6626E-02
1.00357E-02	447.353	1.8132E-02
1.20498E-02	454.1321	2.1489E-02
1.50839E-02	462.1613	2.6514E-02
3.10935E-02	481.5275	5.3324E-02
4.08409E-02	487.6024	6.9871E-02

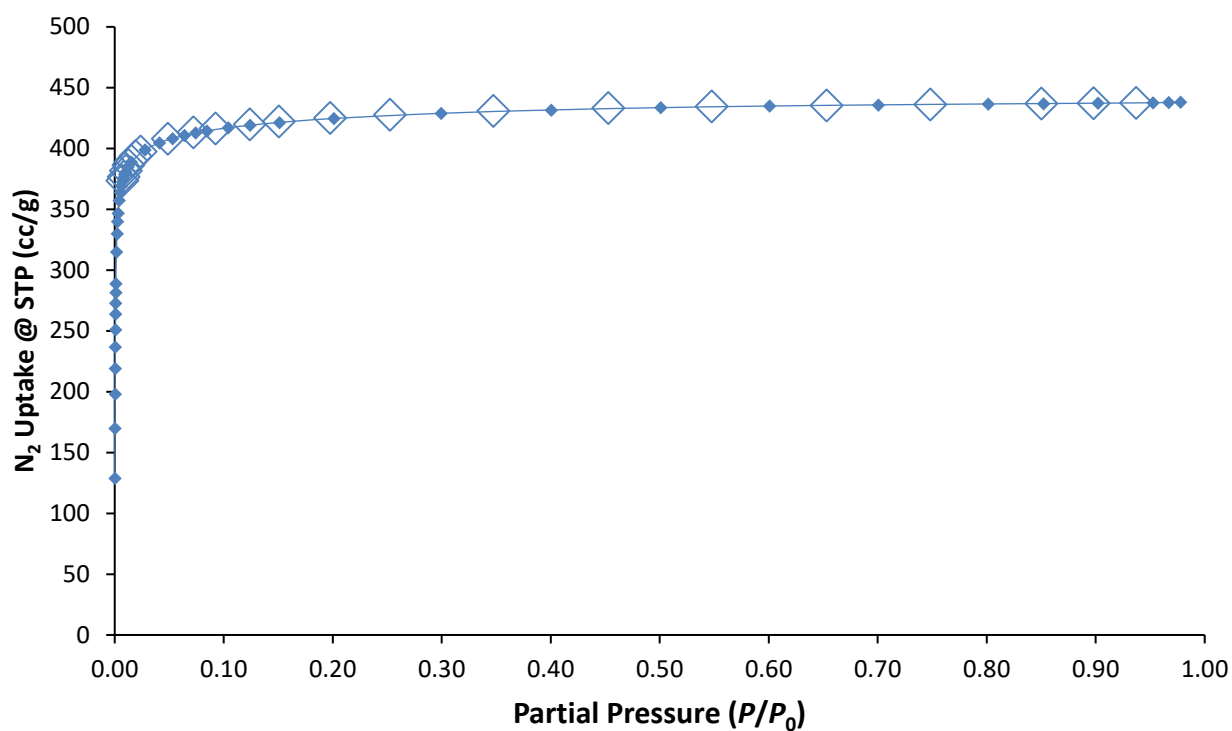


Figure S32: N₂ gas adsorption isotherm at 77 K for **WUF-53**. Adsorption shown in solid diamonds, desorption hollow diamonds. Surface area 1706 m²g⁻¹.

BET summary		WUF-53 20-106
Slope =		2.04
Intercept =		7.906E-04
Correlation coefficient, r =		0.999994
C constant =		2581.097
Surface Area =		1706.535 m ² /g
Relative Pressure P/Po	Volume @ STP (cc/g)	1 / [W((Po/P) - 1)]
8.05463E-03	376.0713	1.7276E-02
9.01998E-03	378.5998	1.9236E-02
9.99859E-03	380.7641	2.1223E-02
1.20633E-02	385.0249	2.5375E-02
1.49766E-02	388.9399	3.1278E-02
2.76786E-02	398.8691	5.7102E-02
4.09897E-02	404.6732	8.4508E-02

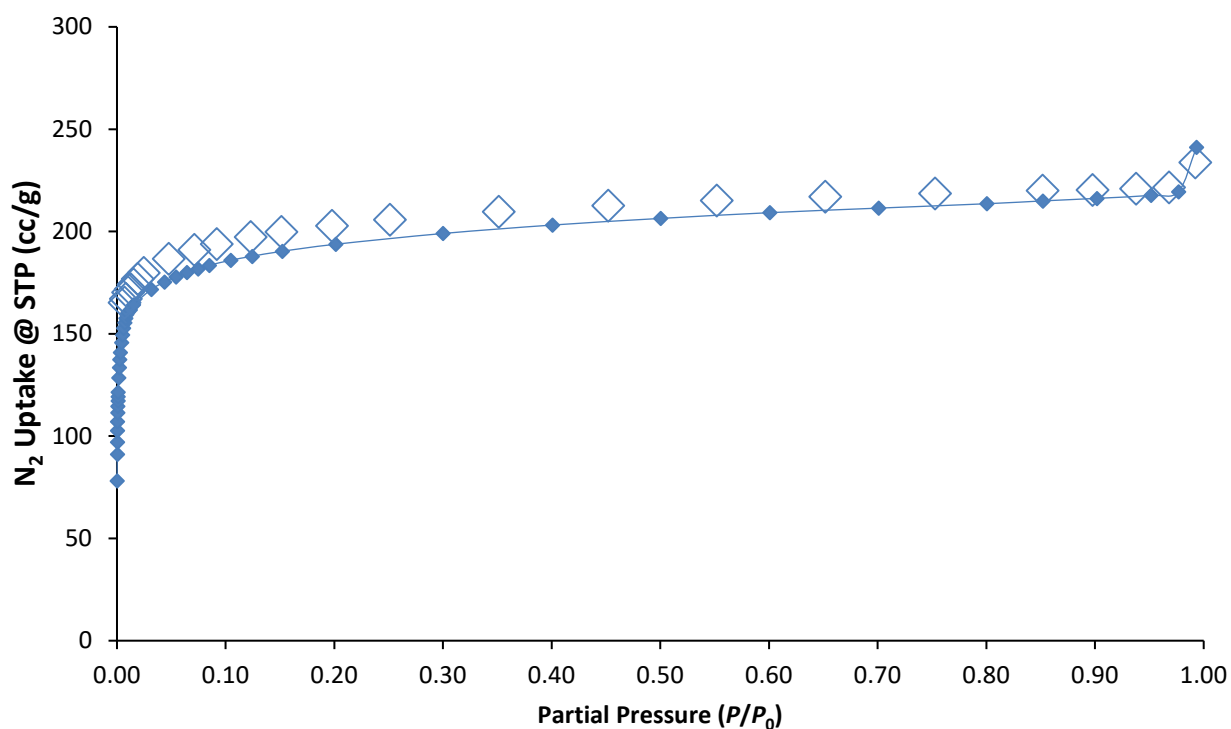


Figure S33: N₂ gas adsorption isotherm at 77 K for PS-**WUF-54**. Adsorption shown in solid diamonds; desorption hollow diamonds. Surface area 741 m²g⁻¹.

BET summary		PS-WUF-54 19-046
Slope =		4.693
Intercept =		3.645e-03
Correlation coefficient, r =		0.999998
C constant =		1288.660
Surface Area =		741.413 m ² /g
Relative Pressure P/Po	Volume @ STP (cc/g)	1 / [W((Po/P) - 1)]
9.96732E-03	160.655	5.0140E-02
1.21357E-02	161.744	6.0770E-02
1.50287E-02	164.1655	7.4365E-02
3.14969E-02	171.665	1.5158E-01
4.36022E-02	175.2725	2.0812E-01
5.41665E-02	177.8109	2.5770E-01
6.44182E-02	179.9283	3.0618E-01